

Optimizing ML Training with Metagradient Descent

Logan Engstrom^{*1}, Andrew Ilyas^{*2†}, Benjamin Chen^{*1},
Axel Feldmann¹, William Moses³, Aleksander Mądry¹

^{*}Equal contribution ¹MIT, ²Stanford, ³UIUC

Abstract

A major challenge in training large-scale machine learning models is *configuring* the training process to maximize model performance, i.e., finding the best training setup from a vast design space. In this work, we unlock a gradient-based approach to this problem. We first introduce an algorithm for efficiently calculating *metagradients*—gradients through model training—at scale. We then introduce a “smooth model training” framework that enables effective optimization using metagradients. With metagradient descent (MGD), we greatly improve on existing dataset selection methods, outperform accuracy-degrading data poisoning attacks by an order of magnitude, and automatically find competitive learning rate schedules.

1 Introduction

How should I clean my data? What architecture should I use? Training large-scale (i.e., deep) machine learning models entails making many design decisions. When making such decisions, typical practice is to exhaustively search over a small set of standard options. For example, we might try a few well-known data cleaning heuristics, construct a grid over a hyperparameters, and choose the options that yield the best models. However, given that this process explores only a small part of the overall design space (e.g., one can construct 2^n possible training datasets from a pool of n candidate datapoints), it is unlikely that this approach really yields the *optimal* training configuration.

How can we find optimal (or at least, better) training configurations? To do so, we take the optimization perspective on designing model training. From this well-studied perspective, deciding on a training configuration—or as we will call it, a set of *metaparameters*—is just a high-dimensional optimization problem. The input space of this problem comprises all possible metaparameter choices, including which datapoints to train on, what model architecture to use, and how to initialize model weights. The objective function takes in a set of metaparameters, trains a machine learning model according to those metaparameters, and then returns a target metric evaluated on that model (e.g., test accuracy). From this perspective, any procedure for selecting metaparameters—including the typical practice of grid-searching over standard options—is just an optimization algorithm, whose goal is to maximize the objective function with respect to the (high-dimensional) input.

Given that selecting metaparameters is “just” a high-dimensional optimization problem, a natural tool to consider is the *gradient*. After all, in many contexts, gradients offer a more effective approach to maximizing high-dimensional functions than grid search. Indeed, for a sufficiently “well-behaved” function $f(x)$ with gradient $\nabla f(x)$, we can optimize f by iteratively updating x in the direction of $\nabla f(x)$. This insight suggests a generic recipe for selecting metaparameters: first, make the objective differentiable with respect to the metaparameters; second, update via gradient steps.

Now, the idea of using gradients to search for metaparameters is not new. Indeed, there is a substantial line of work that aims to optimize metaparameters (e.g., architectures, regularizers, or data augmentation schemes) with gradient-based methods [MDA15; LSY18; LVD20]. However, such methods have not managed to scale beyond relatively small settings. This state of affairs prompts our main question:

Can we scalably configure model training using gradient-based methods?

[†]Work done at MIT EECS. Correspondence to {engstrom, ailyas, benchen}@mit.edu.

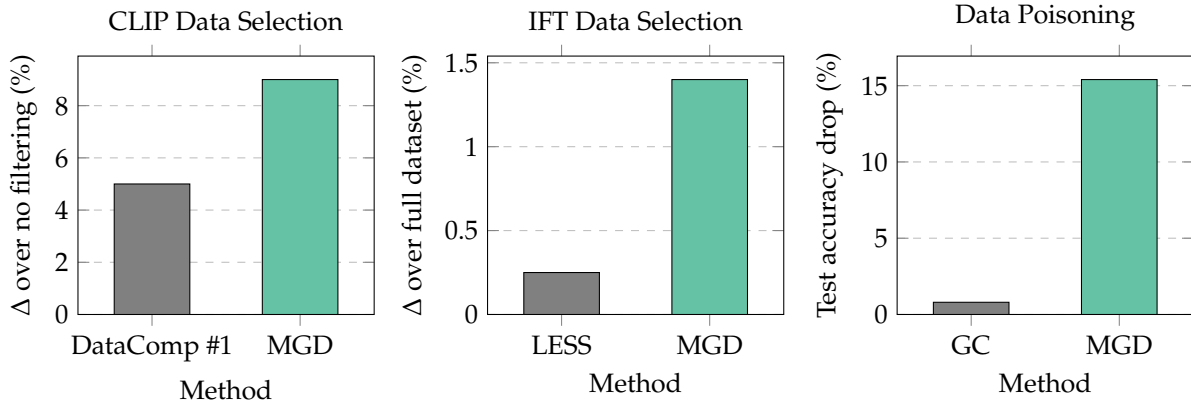


Figure 1: Our proto-algorithm, metagradient descent (MGD), uses gradients to achieve state-of-the-art performance across a variety of applications, including data selection and data poisoning.

1.1 Contributions

In this work, we answer this question in the affirmative, adding “gradient descent on metaparameters” to the large-scale machine learning toolkit. Along the way, we will face—and address—two main challenges.

First, existing methods for computing metagradients do not scale. In response, we devise an algorithm, REPLAY, that can take metagradients in large-scale settings. By combining reverse-mode autodifferentiation (AD) with an efficient data structure, REPLAY can calculate exact metagradients for models with billions of parameters and thousands of training steps.

Second, we find that metagradients of standard training routines are not necessarily helpful for optimization, which we connect to *non-smoothness* of the metaparameter optimization landscape. Borrowing tools from convex optimization, we devise a framework for designing “metasmooth” training routines that *do* admit helpful metagradients.

Addressing the challenges above unlocks a simple recipe for solving a broad range of machine learning tasks: (a) frame the task as a continuous optimization problem over metaparameters; (b) design a metasmooth training routine; (c) perform metagradient descent (MGD). Applying this recipe:

- In the DataComp-sma11 competition [GIF+24], we achieve state-of-the-art pre-training data selection for CLIP (2x larger performance improvement than the previous DataComp-sma11 leader [Eco24]);
- In the context of data selection for instruction tuning (as introduced by Xia et al. [XMG+24]), we substantially improve on data selection for Gemma-2B (outperforming existing selection methods as well as full-data training);
- In the *accuracy-degrading* data poisoning setting (defined by Huber [Hub64] and pioneered by Lu et al. [LKY22] for deep neural networks), we improve attacks on DNNs by an order of magnitude, dropping CIFAR-10 accuracy from 92% \rightarrow 78% (the best previous attack [LKY23] only reduces accuracy to 91%);
- For the task of hyperparameter optimization, we efficiently find a competitive CIFAR-10 learning rate schedule (matching the performance of a schedule found by grid search).

2 Scalably computing metagradients

In this section we present REPLAY, an algorithm for computing metagradients of large-scale iterative ML algorithms. We first detail the setting, then discuss existing approaches to computing metagradients, and conclude by describing REPLAY.

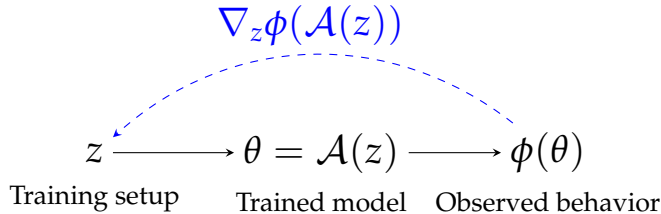


Figure 2: An illustration of the metagradient. We embed a given aspect of the training setup (e.g., the training dataset, or optimizer hyperparameters) into a continuous *metaparameter* vector $z \in \mathbb{R}^d$. This metaparameter defines a model $\mathcal{A}(z)$ by way of the learning algorithm \mathcal{A} , which in turn defines an output $\phi(z)$. The *metagradient* $\nabla_z \phi(\mathcal{A}(z)) \in \mathbb{R}^d$ is the gradient of this model output with respect to the metaparameter.

2.1 What is a metagradient?

Training a machine learning model is a two-step process. First, we decide on a *training setup*—we must pick, for example, a neural network architecture, a training dataset, and an optimizer for training. Second, we apply the algorithm defined by this training setup to train a model.

Our overall goal in this paper is to optimize model behavior as a function of the training setup (or, as we call it, the *metaparameters*) using gradient-based methods. To this end, we define the following notation:

- Let $\mathbf{z} \in \mathbb{R}^n$ be a vector of continuous metaparameters representing the aspects of the training setup we aim to optimize. For example, if we only want to adjust the learning rate and weight decay of SGD then $n = 2$. We handle discrete metaparameters (e.g., choice of training data) by finding a continuous relaxation (e.g., importance weights).
- Let \mathcal{A} be an *algorithm* mapping \mathbf{z} to a trained machine learning model; we assume all other aspects of the training setup outside \mathbf{z} are fixed and thus part of the algorithm \mathcal{A} .
- Finally, let ϕ be an *output function* mapping a model θ to a vector $\phi(\theta) \in \mathbb{R}$. For example, $\phi(\theta)$ might represent the validation loss of the model θ . We require that ϕ be differentiable with respect to θ , but otherwise make no assumptions on ϕ .

With this notation in place, we define the *training function* $f := \phi \circ \mathcal{A}$ mapping the training setup \mathbf{z} *directly* to the output function ϕ evaluated on the corresponding model.

Finally, the *metagradient* is the gradient of the training function with respect to the metaparameters, $\nabla_{\mathbf{z}} f(\mathbf{z})$. Intuitively, the metagradient defines the “direction of steepest ascent” in metaparameter space.

Our focus: iterative algorithms. To efficiently compute the metagradient, we restrict our focus to cases where the algorithm \mathcal{A} is *iterative*, i.e., when it can be written in the form

$$\underbrace{\mathcal{A}(z) := \mathbf{s}_T}_{\text{model state after } T \text{ steps}}, \quad \text{where} \quad \underbrace{\mathbf{s}_{t+1} := h_t(\mathbf{s}_t, \mathbf{z})}_{\text{optimizer step } t}. \tag{1}$$

Here, \mathbf{s}_t is the optimizer state at step t (with \mathbf{s}_0 being the initial state) and h_t is the *update* mapping from state t to state $t + 1$. The form of (1) captures most large-scale training algorithms. For example, if the setup $\mathbf{z} \in \mathbb{R}^T$ is a *per-step* learning rate, and the algorithm \mathcal{A} is full batch gradient descent, then each update h_t is

$$h_t(\mathbf{s}_t, \mathbf{z}) := \mathbf{s}_t - z_t \nabla \ell(\mathbf{s}_t),$$

where z_t is the learning rate at step t , ℓ is the training loss, and the state \mathbf{s}_t comprises the parameters at step t . For more complex algorithms like Adam [KB15], the state \mathbf{s}_t includes terms like gradient moments.

2.2 Warmup: Metagradients via autodifferentiation

A key primitive we leverage to calculate metagradients is *automatic differentiation* (AD)—a standard tool for taking gradients through computer-defined functions. AD takes gradients by decomposing functions into elementary operations with known derivatives, then combining these derivatives using the chain rule. Concretely, AD operates in two passes: a “forward pass,” which executes the function of interest and stores intermediate products for each elementary operation; and a “backward pass,” which calculates the gradient by propagating chains of partial derivatives using these stored products. For the purposes of this paper, we will view AD as a black box that calculates the gradient of a many-to-one function (i.e., any $f : \mathbb{R}^d \rightarrow \mathbb{R}$) at a given point using only a small constant factor more time than calculating the function itself (along with the space cost of storing the necessary forward-pass products).

What does this have to do with metagradients? Well, seeing as how training itself is a computer-defined function, AD is a natural tool for calculating the metagradient. The main challenge, as we discuss in the sequel, is that AD-based approaches to calculating the metagradient tend to be too resource-intensive for the large-scale machine learning algorithms we consider. In the remainder of this section we build up background before finally describing REPLAY, our algorithm for scalably computing (exact) metagradients.

Approach #1: Direct AD. The direct approach to calculating metagradients exploits the fact that nearly any learning algorithm is itself a sequence of differentiable computer-defined operations—meaning the training function f is *also differentiable*.

However, operationalizing this observation to compute metagradients turns out to be challenging. The reason is that AD stores intermediate products for *each* operation. The amount of data stored thus scales with the number of operations in the function of interest. In the case of our training function f , this number encompasses *all* the operations used to train a machine learning model. As a result, even in a toy scenario like MNIST training, computing metagradients with naïve AD would require storing terabytes of data.

Approach #2: Exploiting structure with step-wise AD. A more efficient method for calculating the metagradient, *step-wise AD*, leverages the structure of iterative learning algorithms [Wer90; MDA15; FDF+17]. Recall from (1) that such algorithms take the form

$$\mathcal{A}(\mathbf{z}) := \mathbf{s}_T, \quad \text{where} \quad \mathbf{s}_{t+1} := h_t(\mathbf{s}_t, \mathbf{z}).$$

Algebraic manipulation (in particular, using the chain rule, the law of the total derivative, and the identity $\mathbf{s}_t = h_{t-1}(\mathbf{s}_{t-1}, \mathbf{z})$) allows us to write the metagradient over an iterative algorithm as

$$\frac{\partial f(\mathbf{z})}{\partial \mathbf{z}} = \frac{\partial \phi(\mathcal{A}(\mathbf{z}))}{\partial \mathbf{z}} = \sum_{t=1}^T \underbrace{\frac{\partial \phi(\mathbf{s}_T)}{\partial \mathbf{s}_t}}_{A_t} \cdot \underbrace{\frac{\partial h_{t-1}(\mathbf{s}_{t-1}, \mathbf{z})}{\partial \mathbf{z}}}_{B_t}, \quad (2)$$

where we have introduced the notation A_t and B_t for notational convenience. Step-wise AD computes the metagradient by calculating each term in the sum of (2) one at a time. For each term, the main challenge lies in computing A_t , since given A_t we can straightforwardly compute B_t (the entire term) by differentiating through a single model update, i.e.,

$$B_t := A_t \cdot \frac{\partial h_{t-1}(\mathbf{s}_{t-1}, \mathbf{z})}{\partial \mathbf{z}} = \frac{\partial (A_t \cdot h_{t-1}(\mathbf{s}_{t-1}, \mathbf{z}))}{\partial \mathbf{z}},$$

which is just a single call to our assumed “AD oracle” on the function $\mathbf{z} \mapsto A_t \cdot h_{t-1}(\mathbf{s}_{t-1}, \mathbf{z})$. Computing the A_t terms is less straightforward as we need to relate \mathbf{s}_t and \mathbf{s}_T ; to do so, we exploit the recurrence

$$A_t := \frac{\partial \phi(\mathbf{s}_T)}{\partial \mathbf{s}_t} = \frac{\partial \phi(\mathbf{s}_T)}{\partial \mathbf{s}_{t+1}} \cdot \frac{\partial h_t(\mathbf{s}_t, \mathbf{z})}{\partial \mathbf{s}_t} = \frac{\partial (A_{t+1} \cdot h_t(\mathbf{s}_t, \mathbf{z}))}{\partial \mathbf{s}_t}, \quad (3)$$

making A_t straightforward to compute (again, a single “AD oracle” call) given A_{t+1} . Step-wise AD exploits this fact to successively calculate the gradient with respect to each state, from state T down to state 0.

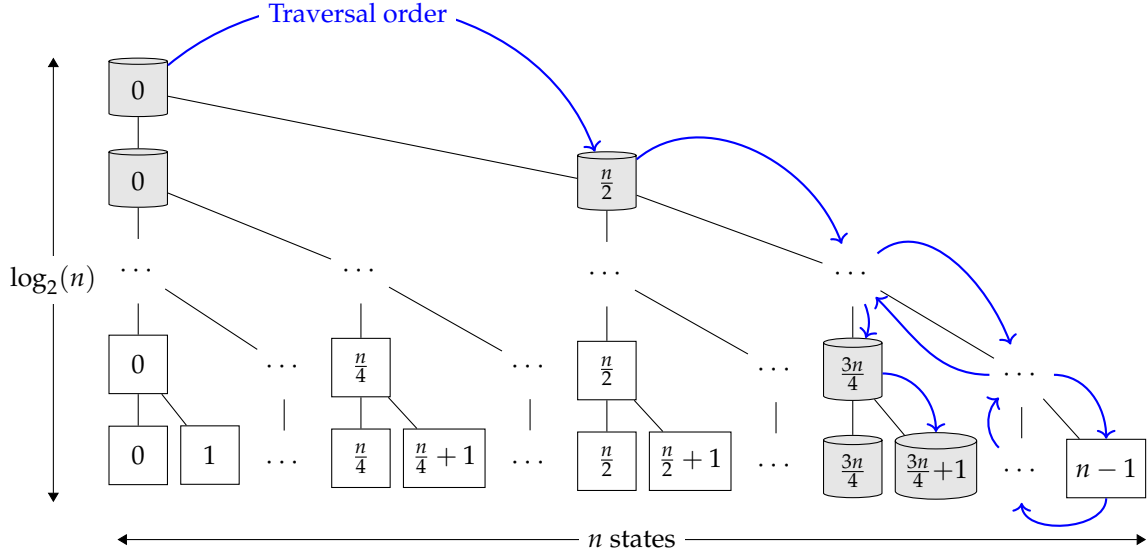


Figure 3: The lazy k -ary tree structure for traversing optimizer states in reverse order, with $k = 2$. Recall that n is the number of states (parameterized such that $n = T + 1$). Each node represents the correspondingly numbered state. We give an example of the traversal using the blue arrows in the figure, which denote the traversal path up to state $s_{\frac{3n}{4}+1}$. The gray cylinders \square indicate the states that are stored when the traversal is at state $s_{\frac{3n}{4}+1}$; the other states are not stored at this point in the traversal. Traversing this structure requires storing $\mathcal{O}(\log(n))$ state and computing $\mathcal{O}(n \log(n))$ optimizer steps—compared to n for simply training.

Bringing these ingredients together, the algorithm executes as follows. As a preprocessing step, it trains the model and stores all intermediate states $\mathbf{s}_0, \dots, \mathbf{s}_T$. Then, the algorithm calculates and sums the terms in (2). It first computes $A_T := \partial\phi(\mathbf{s}_T)/\mathbf{s}_T$, the gradient of the output function ϕ with respect to the final state. Then, the algorithm steps through $\mathbf{s}_{T-1}, \dots, \mathbf{s}_0$ in reverse order, calculating (a) the gradient with respect to each state A_t (via (3)) and (b) the gradient with respect to \mathbf{z} at that step B_t (via (2), using the previously calculated gradient with respect to that state). AD calculates both quantities—each requires differentiating over only one train step. Finally, the algorithm returns the final metagradient as the sum of the terms.

Despite improving storage overhead compared to “direct AD”, step-wise AD is still too space-intensive at scale. After all, this algorithm saves *every* optimizer state.

2.3 REPLAY

REPLAY is our algorithm for efficiently and exactly computing metagradients. It uses $\mathcal{O}(k \log_k(T))$ space and requires running the learning algorithm \mathcal{A} a total of $1 + \log_k(T)$ times, with k a user-chosen constant. The main idea is to make the space-intensive subroutine of step-wise AD—a reverse-order traversal of the optimizer states at each step—much more efficient. After all, step-wise AD stores *all* the states to reverse traverse them. REPLAY modifies step-wise AD to traverse states in less space by exploiting a simple observation: when training is deterministic, one can *reinstantiate* an optimizer state \mathbf{s}_t by “replaying” training from a fixed point $t' < t$ —at the compute cost of $t - t'$ training steps. For example, one simple scheme saves every other state, then “replays” the remaining states when (reverse) traversing; this routine stores $T/2$ states but computes an extra $T/2$ model updates compared to storing *all* the states.

REPLAY performs a reverse-order traversal the optimizer states while balancing the compute cost of “replaying” training with the storage cost of saving states. We use a combination of deterministic training (fixing data ordering, data augmentation, and any other randomness in the training process) and an efficient data structure (similar to a segment tree; see Figure 3) to reverse-order traverse the optimizer states with $\mathcal{O}(k \log_k(T))$ space and an additional $T \log_k(T)$ model steps.

Specifically, REPLAY recursively saves and replays training states. The algorithm splits the training trajectory into k segments, performs the full training routine while saving only the start of each segment, then recurses into each segment (in reverse) to retrieve the states in reverse-order. The recursion depth bottoms out at $\log_k(T)$, at which point the algorithm has k consecutive optimizer states in memory; the algorithm then backpropagates along this segment, before deleting all these states from memory and then reinstantiating the next k -length segment of optimizer states. We provide additional details on the algorithm in Appendix A.2. REPLAY unlocks computing large-scale metagradients by requiring only logarithmic storage and additional compute time.

Remark 1 (Connection to rematerialization). *In a broad sense, both REPLAY and step-wise AD above can be viewed as special cases of a classical approach in AD (and computing broadly) known as rematerialization [CAC+81; BCT92; ZP00; GW08; CXZ+16]. To our knowledge, however, REPLAY is the first application of this particular rematerialization technique to the problem of computing metagradients through model training.*

Remark 2 (Reversible learning). *An alternative approach to calculating metagradients that does not save any state is reversible learning [MDA15], for which one can “invert” previous training states from future ones. We focus here on general (non-reversible) learning algorithms for two reasons: first, even simple algorithms such as SGD without momentum are non-reversible; second, reversibility in practice introduces numerical precision issues.*

3 Designing metasmooth training routines

Given a training function f , REPLAY enables us to compute metagradients $\nabla f(\mathbf{z})$ for any setup \mathbf{z} . Can we immediately use these metagradients to optimize model training setups? The answer is (generally) no: we find that applying REPLAY to a function f representing a standard model training and evaluation routine yields metagradients that are often $\pm\infty$ -valued and generally unhelpful for optimization. Indeed, previous work has observed similar issues optimizing over even (very) small-scale training [BSF94; Pea96; MDA15].

In this section, we show that an underlying source of the issue is the landscape of the metaparameter optimization problem. We then present a framework for modifying standard learning algorithms to admit useful metagradients, i.e., to be *metasmooth*. To use a familiar analogy: just as residual connections and improved initialization schemes can improve optimization in standard deep learning algorithms, our framework introduces an analogous set of modifications to enable optimization with metagradients.

3.1 The metaparameter optimization landscape

We first review the notion of smoothness from optimization theory, and then adapt it to the setting of metagradients. The resulting *metasmoothness* metric allows us to quantify (and later, improve) the amenability of the metaparameter optimization problem to gradient-based methods.

Smoothness. In optimization theory, the basic property of a function that controls how effectively it can be optimized with first-order methods is *smoothness*. Specifically, a function $f(\mathbf{z})$ is β -smooth at a point \mathbf{z} if its gradient ∇f satisfies the property that

$$\|\nabla f(\mathbf{z}) - \nabla f(\mathbf{z}')\| \leq \beta \cdot \|\mathbf{z} - \mathbf{z}'\| \quad \text{for all } \mathbf{z}', \quad (4)$$

or in other words, if its gradient does not change too quickly around \mathbf{z} . To motivate this definition: if a function f is β -smooth at \mathbf{z} , then a step of gradient descent with step size $1/\beta$ will successfully decrease the value of the function:

$$f\left(\mathbf{z} - \frac{1}{\beta}\nabla f(\mathbf{z})\right) \leq f(\mathbf{z}) - \frac{1}{2\beta}\|\nabla f(\mathbf{z})\|^2.$$

This guarantee makes β -smoothness a good measure of gradient utility.

Metasmoothness. There are two main challenges in adapting the smoothness property to the metagradient setting. First, evaluating (4) requires a search over all possible \mathbf{z}' , which is infeasible. Second, even if we could exactly evaluate the left-hand side of (4), it would be difficult to disentangle non-smoothness of the training function f from potential error in metagradient computation (e.g., a numerically unstable operation in REPLAY).

To sidestep these issues, we propose a metric called *metasmoothness*, given in Definition 1. Metasmoothness is cheap to compute—requiring only three evaluations of the training function—and does not rely on metagradient computation. For the remainder of this section, we fix a small constant $h > 0$, and define the corresponding finite-differences estimator of the directional derivative Δ_f as

$$\Delta_f(\mathbf{z}; \mathbf{v}) := \frac{f(\mathbf{z} + h\mathbf{v}) - f(\mathbf{z})}{h}.$$

Definition 1 (Metasmoothness of f at \mathbf{z} towards \mathbf{v}). Consider a training function f mapping metaparameters $\mathbf{z} \in \mathbb{R}^n$ to model output $f(\mathbf{z}) \in \mathbb{R}$. Given a metaparameter \mathbf{z} and a vector $\mathbf{v} \in \mathbb{R}^n$, the metasmoothness of f at \mathbf{z} towards \mathbf{v} is given by

$$S_{h,\mathbf{v}}(f; \mathbf{z}) := \left| \frac{\Delta_f(\mathbf{z} + h\mathbf{v}) - \Delta_f(\mathbf{z})}{h} \right|. \quad (5)$$

Definition 1 measures the rate of change of the derivative of $f(\mathbf{z})$ in the direction of a given vector \mathbf{v} , and is therefore related to β -smoothness in that:

- (a) If f is β -smooth at \mathbf{z} , then $S_{h,\mathbf{v}}(f; \mathbf{z}) \leq \beta$ for any (h, \mathbf{v}) (so Definition 1 is *necessary* for smoothness).
- (b) If $\lim_{h \rightarrow 0} S_{h,\mathbf{v}}(f; \mathbf{z}) \leq \beta$ for all $\mathbf{z} \in \mathbb{R}^n$ and $\mathbf{v} \in \mathbb{S}^{n-1}$, then f is β -smooth everywhere (so a global version of Definition 1 is *sufficient* for smoothness).

Empirical metasmoothness. Definition 1 lets us measure the meta-smoothness of a training function f at a particular metaparameter \mathbf{z} (towards a direction \mathbf{v}). This definition, however, has two shortcomings. First, recall that the training function f is a composition of a learning algorithm \mathcal{A} and an output function ϕ , so the smoothness of f depends on that of both \mathcal{A} and ϕ (in particular, $\partial f / \partial \mathbf{z} = \partial \phi / \partial \mathcal{A} \cdot \partial \mathcal{A} / \partial \mathbf{z}$). Since the output function ϕ might be unknown ahead of time, we are most interested in measuring the *overall* metasmoothness of a learning algorithm \mathcal{A} . Second, while the result of (5) does have a concrete basis in optimization theory, it may not be easy to interpret in practice (e.g., what does $S = 200$ mean?). We address both issues simultaneously by (a) proposing an interpretable “binarized” version of Definition 1, and (b) studying metasmoothness in the space of model parameters θ , instead of the output space.

Definition 2 (Empirical metasmoothness of \mathcal{A}). Let \mathcal{A} be a learning algorithm which maps metaparameters $\mathbf{z} \in \mathbb{R}^n$ to model parameters $\theta \in \mathbb{R}^d$, let \mathbf{z} be a metaparameter vector, and let \mathbf{v} be a given direction. Let $\mathbf{d} \in \mathbb{R}^d$ be the per-coordinate variation in θ , i.e.,

$$\mathbf{d} = |\mathcal{A}(\mathbf{z} + 2h\mathbf{v}) - \mathcal{A}(\mathbf{z})|$$

The empirical (h, \mathbf{v}) -metasmoothness of \mathcal{A} at \mathbf{z} is given by

$$\widehat{S}_{h,\mathbf{v}}(\mathcal{A}; \mathbf{z}) = \text{sign}(\Delta_{\mathcal{A}}(\mathbf{z}; \mathbf{v}))^\top \cdot \text{diag} \left(\frac{\mathbf{d}}{\|\mathbf{d}\|_1} \right) \cdot \text{sign}(\Delta_{\mathcal{A}}(\mathbf{z} + h\mathbf{v}; \mathbf{v})), \quad (6)$$

weights each parameter by its range.

Intuitively, (6) measures the agreement in sign between the (finite-difference approximation of the) metagradient in the direction of \mathbf{v} at \mathbf{z} and at $\mathbf{z} + h\mathbf{v}$, averaged across parameter coordinates and weighted by the variation in each coordinate. Taking a weighted average of sign agreements ensures that $\widehat{S} \in [-1, 1]$ (making it easier to interpret than Definition 1). The $\text{diag}(\mathbf{d}/\|\mathbf{d}\|_1)$ term weights each agreement proportionally to the scale of the corresponding parameter change (downweighting, e.g., coordinates i that are essentially constant). Finally, observe that Definition 2 is efficient to compute in practice: it requires only three calls to the learning algorithm \mathcal{A} .

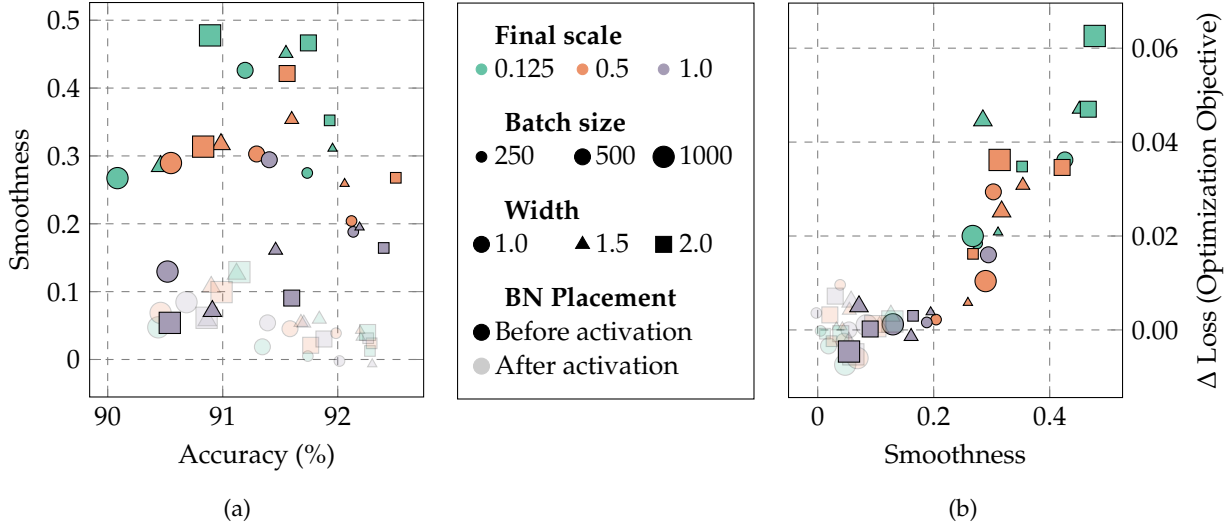


Figure 4: (a) For a variety of training configurations of a ResNet-9 model, we plot metasmoothness (Def. 2) against test accuracy. Strategies such as increasing width, placing batch normalization before activations, and scaling down network outputs consistently improve metasmoothness, at a minor cost to accuracy. (b) Smoother training configurations can be optimized via metagradients more effectively. Here, as in Section 4.3, we use metagradients to gradient ascend on validation loss.

Remark 3. Ideally, recalling the smoothness definition (4), we would evaluate metasmoothness in all possible directions \mathbf{v} and all points \mathbf{z} . Empirically, we find in the sequel (Section 3.2) that this single-direction approximation at a single point \mathbf{z} still yields a useful estimate of metasmoothness (e.g., one that correlates with metagradient utility).

3.2 Estimating and improving metasmoothness

Having established a method for quantifying metasmoothness, we turn to the practical question: how can we design learning algorithms that are amenable to metagradient optimization? To answer this question, we introduce a straightforward framework: given a learning algorithm, explore a fixed menu of possible modifications to the training setup, and choose the combination that maximizes empirical metasmoothness. In practice, we find that this framework allows us to slightly modify learning algorithms in a way that makes them amenable to first-order methods.

As a case study, we study the task of training ResNet-9 on the CIFAR-10 dataset [Kri09]. We let the metaparameters \mathbf{z} be a perturbation to the pixels of 1000 random training images (so $\mathbf{z} \in \mathbb{R}^{1000 \times 32 \times 32 \times 3}$). We estimate the empirical metasmoothness of different learning algorithms \mathcal{A} at $\mathbf{z} = \mathbf{0}$ using Definition 2. Concretely, we proceed as follows for each learning algorithm \mathcal{A} :

1. Let $\mathbf{z}_0 = \mathbf{0}$ be the metaparameter corresponding to the original dataset.
2. Sample a random perturbation vector $\mathbf{v} \sim \mathcal{N}(0, 1)$.
3. Compute the empirical metasmoothness (6), i.e.,
 - (a) Let $\theta_0 := \mathcal{A}(\mathbf{z}_0)$, $\theta_h := \mathcal{A}(\mathbf{z}_0 + h \cdot \mathbf{v})$, and $\theta_{2h} := \mathcal{A}(\mathbf{z}_0 + 2h \cdot \mathbf{v})$ be the model parameters that result from training with training dataset perturbations \mathbf{z}_0 , $\mathbf{z}_0 + h\mathbf{v}$, and $\mathbf{z}_0 + 2h\mathbf{v}$, respectively.
 - (b) Compute the approximate derivatives

$$\Delta_{\mathcal{A}}(\mathbf{z}_0; \mathbf{v}) = (\theta_h - \theta_0) / h, \quad \Delta_{\mathcal{A}}(\mathbf{z}_0 + h\mathbf{v}; \mathbf{v}) = (\theta_{2h} - \theta_h) / h.$$

- (c) Compute the weighting vector $\mathbf{d} = |\theta_{2h} - \theta_0|$, and compute the average metasmoothness (6), i.e.,

$$\hat{S}_{h, \mathbf{v}}(\mathcal{A}; \mathbf{z}_0) = \text{sign}(\Delta_{\mathcal{A}}(\mathbf{z}_0 + h\mathbf{v}; \mathbf{v}))^\top \cdot \text{diag} \left(\frac{\mathbf{d}}{\|\mathbf{d}\|_1} \right) \cdot \text{sign}(\Delta_{\mathcal{A}}(\mathbf{z}_0; \mathbf{v})).$$

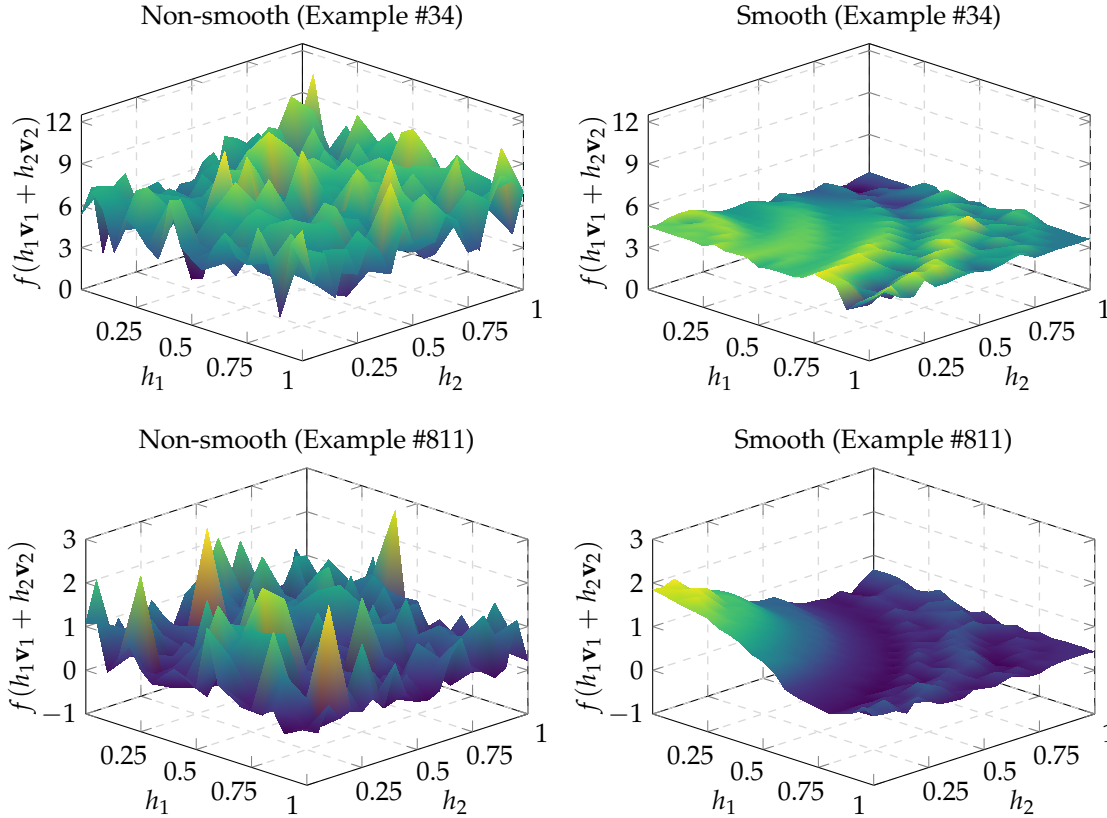


Figure 5: The effect of metasmoothness on the optimization landscape. Each plot above visualizes the loss landscape of a (deterministic) learning algorithm \mathcal{A} , with the x - and y -axes representing additive perturbations to 1000 examples in the training set and the z -axis representing the resulting model’s loss on the test example given in the title. In each row, the left plot is a non-smooth algorithm, and the right plot is a smooth algorithm (as per Definition 2) evaluated on the same example. Overall, empirical metasmoothness seems to strongly correlate with qualitative landscape smoothness. See Figure 12 for more examples.

Metasmooth learning algorithms. We apply the procedure above to estimate the metasmoothness of learning algorithms induced by different design choices (batch size, network width, BatchNorm placement, gradient scaling), and report the results in Figure 4 (left). On one hand, “standard” learning algorithms (i.e., those designed without metasmoothness in mind) are not metasmooth. On the other hand, our investigation reveals central factors driving metasmoothness. In addition to “standard” hyperparameters such as batch size and network width playing a role, we find that placing Batch Normalization layers *prior* to nonlinearities (instead of after) and scaling the final layer output are both crucial to metasmoothness. Note that the modifications we consider above are not exhaustive—see Appendix E for the full training setup.

Finally, in Figure 5, we plot the optimization landscape of both metasmooth (right) and non-metasmooth (left) models. We find that the landscapes of metasmooth models are much smoother and—qualitatively—more straightforward to optimize.

Metasmoothness/performance tradeoffs? Figure 4 (left) relates metasmoothness to model accuracy for the considered learning algorithms. While there is no clear trend, the top-performing learning algorithms are not always metasmooth. However, the trade-off is not too severe: the most metasmooth algorithms still achieve near-optimal accuracy. Furthermore, it is possible that with additional searching we could identify even more accurate metasmooth models. Taken together with our previous experiment, our results suggest that jointly searching over metasmoothness and model accuracy is a general recipe for designing learning algorithms that are both performant and metasmooth. Finally, as we discuss in Section 5, a fruitful avenue

for future work may be to design metasmooth learning algorithms directly, i.e., without relying on stability heuristics or grid search.

Does metasmoothness aid downstream optimization? Recall that our motivation for studying metasmoothness is to develop learning algorithms that we can optimize the metaparameters of via metagradients (using first-order methods). We started with the notion of β -smoothness from optimization theory, and we adapted it to the setting of metagradients by making a series of approximations and modifications. The final question we address is: does our final notion of metasmoothness actually predict the utility of metagradients for optimization? Figure 4 (right) demonstrates that metasmoothness strongly predicts our ability to optimize the metaparameters of a given learning algorithm. We use metagradients (computed by REPLAY) to gradient ascend on validation loss with respect to the metaparameters \mathbf{z} , and measure the change in model loss.

4 Applications

In this section, apply metagradients to three problems in machine learning: selecting training data, poisoning training data, and searching for hyperparameters. In each setting we follow the same recipe: we frame the task as an optimization problem, modify the learning algorithm of interest to be *smooth*, then solve by first-order optimizing with meta-gradients—which we refer to, in a catch-all manner across algorithms, as metagradient descent (MGD). In particular: we substantially improve on existing dataset selection methods (Section 4.1, Section 4.2), perform the first effective accuracy-degrading data poisoning attack (Section 4.3), and discover one-cycle learning rate schedules with MGD (Section 4.4).

4.1 Selecting multimodal training data

Curating a training dataset from a mass of unfiltered data is a necessary and influential step in any large-scale machine learning pipeline. Deciding how to curate such a dataset is a challenging problem that has attracted substantial recent interest [FIW+22; ATS+23; EFM24; GIF+24]. In this section, we frame pre-training data selection as an optimization problem, and then solve this problem by first-order optimizing with metagradients. Applying our method to the DataComp-small benchmark [GIF+24], we greatly improve on the state-of-the-art (our improvement over state-of-the-art is roughly the same as the improvement of state-of-the-art over training on random data).

4.1.1 Setup

The goal of dataset selection is to choose a training data subset (out of a broad pool of data) that maximizes trained machine learning model performance. Given this goal, dataset selection has a natural interpretation as a combinatorial metaparameter optimization problem. In particular, in the language of Section 2.1, for a training set of size n , let

- (a) the metaparameters $\mathbf{c} \in \mathcal{C} := \mathbb{Z}_{\geq 0}^n$ be non-negative data counts representing the number of times each training sample repeats in the training data;
- (b) the algorithm \mathcal{A} be a standard large-scale learning procedure, which runs on a training set comprising c_i copies of each sample i for $i \in [n]$;
- (c) the output function ϕ be the loss of the trained model on a target distribution D .

Then, defining $f(\mathbf{c}) := \phi(\mathcal{A}(\mathbf{c}))$ (as in Section 2.1), our goal is to find the data counts \mathbf{c}^* that solve

$$\mathbf{c}^* := \arg \min_{\mathbf{c} \in \mathcal{C}} f(\mathbf{c}). \tag{7}$$

4.1.2 Gradient descent on training data

Metagradients let us *directly* minimize the target task loss (7) with respect to the choice of training data. At a high level, our algorithm operates as follows: we start with a randomly chosen set of training data, then iteratively update the dataset selection using metagradients with respect to importance weights placed on each training datapoint. The specifics of our method are in Algorithm 1; we describe its core ideas below.

Idea 1: A surrogate algorithm. We cannot use metagradients to optimize (7) directly, because the meta-parameters of interest \mathbf{c} are discrete counts (and so the algorithm \mathcal{A} is non-differentiable with respect to \mathbf{c}). To circumvent this problem, we relax \mathcal{A} : we define a surrogate algorithm $\mathcal{A}'_{\mathbf{c}}$ that takes in a *continuous* metaparameter $\mathbf{z} \in \mathbb{R}^n$, whose metagradient we *can* compute, then optimize using the metagradient on $\mathcal{A}'_{\mathbf{c}}$.

This surrogate learning algorithm $\mathcal{A}'_{\mathbf{c}}$ maps a metaparameter $\mathbf{z} \in \mathbb{R}^n$ (representing a perturbation to training data weights) to a machine learning model. The surrogate is defined by a set of counts $\mathbf{c} \in \mathbb{Z}_+^n$, and a hyperparameter k denoting a specific training iteration, both of which we bake into the surrogate algorithm itself. Given a metaparameter $\mathbf{z} \in \mathbb{R}^n$, the algorithm $\mathcal{A}'_{\mathbf{c}}$ trains a model “as usual” using the fixed counts \mathbf{c} . That is, it makes c_i copies of each training sample i , shuffles and partitions the data into batches, and then at each iteration minimizes the batch loss with a step—just as the original learning algorithm \mathcal{A} . At iteration k , however, in addition to the original loss on the k -th batch, the algorithm upweights *each* training sample i according to the metaparameter z_i . In other words, the objective at iteration t of the surrogate algorithm $\mathcal{A}'_{\mathbf{c}}$ is

$$\ell'_t(\theta) := \begin{cases} \sum_{x \in t^{\text{th}} \text{ batch}} \ell(x; \theta) & \text{if } t \neq k \\ \sum_{x \in t^{\text{th}} \text{ batch}} \ell(x; \theta) + \sum_{i=1}^n z_i \ell(x_i; \theta) & \text{if } t = k \end{cases}$$

where $\ell(x; \theta)$ is the training loss on example x .

Observe that when $\mathbf{z} = \mathbf{0}_n$, the algorithm $\mathcal{A}'_{\mathbf{c}}$ is identical to the standard learning algorithm \mathcal{A} . And while \mathcal{A} was a function of (nondifferentiable) discrete data counts \mathbf{c} , $\mathcal{A}'_{\mathbf{c}}$ is differentiable with respect its input \mathbf{z} , and so we can compute the metagradient

$$\mathbf{g} := \nabla_{\mathbf{z}} \phi(\mathcal{A}'_{\mathbf{c}}(\mathbf{z})) \Big|_{\mathbf{z}=\mathbf{0}_n}.$$

Intuitively, the entries of the metagradient \mathbf{g} capture the effect of adding an infinitesimal amount of each training sample i to the training data at iteration k . A positive entry g_i indicates that adding an infinitesimal amount of sample i to the training data would increase the loss, and a negative entry indicates that adding an infinitesimal amount of sample i to the training data would decrease the loss; the slot at i represents the (estimated) effect of adding a copy of sample i to the training data at every batch containing the sample.

Idea 2: Block coordinate descent. We then use the metagradient \mathbf{g} to iteratively update our selected dataset. We update data counts as

$$\mathbf{c} \leftarrow \mathbf{c} - \text{sign}(\mathbf{g}) \odot \mathbf{m}, \quad \mathbf{m} \sim \text{Bernoulli}(p), \tag{8}$$

where p is a hyperparameter controlling the fraction of sample counts to update. This algorithm resembles a block coordinate descent algorithm [OR00], with the main difference being that we take signed gradient steps with step size 1 (projected onto non-negative integers) to ensure that the counts remain well-defined. As a result, p implicitly controls the algorithm’s step size.

Applying (8) concludes a single optimization step. By repeating this process of estimating the metagradient, updating our counts vector, then constructing a new training dataset, we iteratively improve the selected data. Pseudocode for our algorithm can be found in Algorithm 1.

4.1.3 Results

We evaluate our data selection algorithm using DataComp [GIF+24], a standardized framework for evaluating data selection methods for multimodal models. Algorithm 1 greatly improves on the state-of-the-art for the benchmark. Below, we describe the setting, outline our method, and conclude with our results.

Algorithm 1: Dataset selection using using metagradient descent (MGD).

Input: initial data counts $\mathbf{c} \in \mathbb{Z}_{\geq 0}^n$, learning algorithm \mathcal{A} , output function ϕ
Hyperparameters: step size p , # opt steps T , iteration number k

- 1 **for** $t \leftarrow 1$ **to** T **do**
- 2 $\mathbf{z} \leftarrow \mathbf{0}_n$ // Build input to surrogate
- 3 $\mathbf{g} \leftarrow \frac{\partial \phi(\mathcal{A}'(\mathbf{z}))}{\partial \mathbf{z}}$ // Calculate metagradient using REPLAY
- 4 $\mathbf{m} \leftarrow$ sample from Bernoulli(p) // Sample indices to step on
- 5 $\mathbf{c} \leftarrow \mathbf{c} - \text{sign}(\mathbf{g}) \odot \mathbf{m}$ // Take optimization step
- 6 **Return** \mathbf{c} // Return final data counts

Setting. DataComp [GIF+24] is a multimodal model training competition and benchmark for evaluating dataset selection methods. DataComp provides a *fixed* learning algorithm chosen in advance by the organizers and a large fixed *candidate pool* of internet data. The goal is to choose a subset of the candidate pool—possibly with repeated datapoints—that yields the best-performing model after training with the given learning algorithm, as measured by a predetermined set of 38 benchmarks. Given a submission subset, the mean score on the evaluation datasets for a model trained with that subset is taken as the final “score.” DataComp offers four separate “scales” requiring different amounts of compute; we focus on the *small* scale in this paper due to compute limitations.

Method. We select data with MGD (Algorithm 1) to minimize loss on data on a “target set” that is distributionally similar to the DataComp benchmark tasks, and select hyperparameters with a held-out “validation set.” In particular, we construct target and validation sets by taking samples from the DataComp evaluation tasks with extra samples available beyond those used in the DataComp test set (e.g., ImageNet, one of the tasks in DataComp, has a training set in addition to the test set evaluated in DataComp). See Appendix C for the exact details of the target and validation sets, the precise hyperparameters used with Algorithm 1, and a discussion on scalability (including further engineering details on executing our algorithm efficiently).

Results. MGD greatly outperforms the current state-of-the-art: the difference in accuracy between MGD and the current best method is roughly as large as the difference between the previous state-of-the-art (EcoDatum [Eco24]) and training on randomly chosen data (cf. Figure 6). Inspecting scores over the course of the optimization in Figure 6, we find that only a few steps are necessary to outperform previous methods.

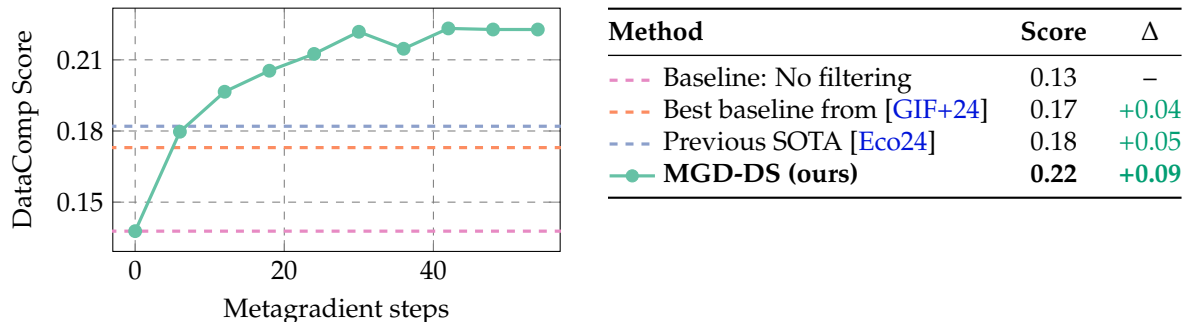


Figure 6: MGD dataset selection greatly outperforms existing methods (improving over the previous SOTA by as much as the previous SOTA improves over no filtering at all). We compare DataComp scores for MGD (over optimization steps), training on the entire candidate pool, the best baseline originally proposed by DataComp, and the previous SOTA [Eco24].

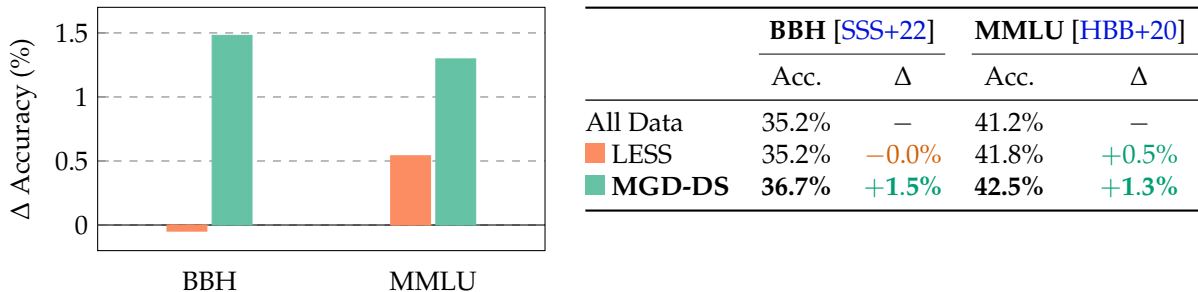


Figure 7: MGD dataset selection outperforms baselines. Comparing to training on all the data: it achieves over double the margin of improvement of LESS on MMLU, and improves by +1.5% on BBH (where LESS does not improve at all). The Δ column denotes improvement over not filtering.

4.2 Selecting instruction-tuning data

In our second application, we select training data for instruction fine-tuning (IFT) using the same MGD-based method detailed in Algorithm 1 of Section 4.1. As with multimodal data, training on the “right” post-training data (such as the “right” IFT data) can greatly impact deployment-time model performance [LFX+24; DJP+24; TGZ+23]. MGD improves over baselines at choosing IFT data for MMLU [HBK+21], a general knowledge task, and BBH [SSS+22], a reasoning/chain-of-thought task.

To overview this section: we start by detailing the setting, then describe the specifics of our MGD instantiation before concluding with results.

Setting. We adopt the setting of LESS [XMG+24]. Here, the goal is to select a training data subset from four combined IFT datasets (Flan V2 [LHV+23], CoT [WWS+22], DOLLY [CHM+23], and Open Assistant 1 [KKR+24]) to maximize accuracy on a given target task. We consider two target tasks from LESS: MMLU (which comprises multiple choice questions spanning a variety of disciplines) and BBH (a 23 task subset of BIG-Bench [SRR+22]). In this setup, the data selector can access samples from each task built from the in-context learning prompts. Following Xia et al. [XMG+24], we fine-tune a 128-width LoRA [HY20] (in our work, on Gemma-2B [TMH+24]). See Appendix D for full details on the tasks and learning algorithm.

Method. We split up the available task samples into two sets—a “target” set and a “validation” set—then select data with MGD (via Algorithm 1) by minimizing causal language modeling loss on the “target” set of samples. We select hyperparameters like step size and number of SGD iterations with the validation set; see Appendix D for more details.

Results. Comparing with two baselines—training on *all* the data and training with data selected with LESS [XMG+24]—MGD yields strictly better training dataset selections for each target task (cf. Figure 7). MGD improves most on BBH, a reasoning task, compared to the best baseline (+1.5% accuracy). On MMLU, a knowledge-based task, we outperform baselines by slightly less compared to the best baseline (+0.8%); one explanation is that selecting IFT data lends more control over reasoning than over intrinsic knowledge available in the LM.

Beyond raw accuracy, we inspect losses across each step of the optimization process. Overall, our method improves validation loss over MGD steps (cf. Appendix Figures 13), but also exhibits signs of overfitting. Given intuition from overparameterized learning, we might expect this behavior: we optimize a total of 270,679 “weights”—each corresponding to a count for a datapoint—to minimize loss on only a handful of test samples (cf. Table 3).

4.3 Accuracy-degrading (Huber) data poisoning

The goal of an accuracy-degrading *data poisoning* attack is to degrade the performance of a machine learning model by corrupting a small fraction of its training data. Here, the considered threat model is as follows.

The attacker is given a training set $\mathbf{X} = \{x_1, \dots, x_n\}$ drawn from a distribution P , and a function $\theta(\cdot)$ mapping training data to model parameters (representing the learning algorithm used by the victim). The attacker’s goal is to return a new training set \mathbf{X}' that differs from \mathbf{X} in at most $\varepsilon \cdot n$ datapoints while inducing model parameters $\theta(\mathbf{X}')$ that perform as poorly as possible on a freshly drawn test set T from P .

Formally, the adversary aims to solve the following optimization problem:

$$\arg \max_{\tilde{x}_1, \dots, \tilde{x}_{n_p}} \mathbb{E}_{x \sim P}[\ell(x; \theta(\mathbf{X}'))], \quad (9)$$

where $\mathbf{X}' = \{\tilde{x}_1, \dots, \tilde{x}_{n_p}, x_{n_p+1}, \dots, x_n\}$ and $n_p = \lfloor \varepsilon n \rfloor$. Note that our goal is to degrade the *overall* model performance on a test set \mathbf{X}_{test} drawn from P (in particular, the test set \mathbf{X}_{test} is *unknown* to the adversary). In this way, this setting resembles the Huber contamination model in statistics [Hub64], and is strictly more challenging than the usual data poisoning settings in deep learning (e.g., backdoor attacks [GDG17] or attacks that target specific test examples [KL17]).

For large-scale machine learning models, finding strong adversaries has proven challenging—standard loss-minimizing learning algorithms seem quite robust to maliciously-inserted data [LKY23]. In fact, the first non-trivial accuracy degradation data poisoning attacks on deep models were pioneered by Lu et al. [LKY22] and later improved upon by the same set of authors [LKY23]. Broadly speaking, even constructing attacks that degrade the overall performance of a learning algorithm by more than the adversarial budget ε has proven challenging.

4.3.1 Setup

We observe that (9) is a continuous optimization problem to which we can directly apply our metagradient framework, approximating the expectation over P by a finite-sample average over a validation set \mathbf{X}_{val} . In particular, given a (randomly shuffled) training set \mathbf{X} and validation set \mathbf{X}_{val} , we set up the following metaparameter optimization problem (see Section 2.1):

- (a) the metaparameter $\mathbf{z} \in \mathcal{X}^{n_p}$ is a tensor of $n_p = \lfloor \varepsilon n \rfloor$ poisoned samples;
- (b) the algorithm \mathcal{A} maps metaparameters \mathbf{z} to a trained model $\mathcal{A}(\mathbf{z})$ by replacing the first¹ n_p samples in \mathbf{X} with the samples in \mathbf{z} and then training on the resulting dataset;
- (c) the output function ϕ evaluates average loss on the validation set \mathbf{X}_{val} .

4.3.2 Algorithm

To apply our first-order methods to this problem, we start by initializing the poisoned data to be exactly the first n_p samples in \mathbf{X} , $\mathbf{z}^{(0)} := \{\tilde{x}_i^{(0)} = x_i : i \in [n_p]\}$. Then, for $t = 1, \dots, T$, we sample a minibatch $\mathbf{X}_{val}^{(t)}$ from \mathbf{X}_{val} and use REPLAY to compute the metagradient

$$\mathbf{g}_t = \frac{d}{d\mathbf{z}} \left(\sum_{x \in \mathbf{X}_{val}^{(t)}} \ell(x; \mathcal{A}(\mathbf{z}^{(t-1)})) \right),$$

and update the poisoned data using (projected) gradient ascent:

$$\mathbf{z}^{(t)} = \Pi_{\mathcal{X}} \left(\mathbf{z}^{(t-1)} + \eta \cdot \text{sign}(\mathbf{g}_t) \right),$$

where $\Pi_{\mathcal{X}}$ is the projection operator onto the sample space \mathcal{X} . (For example, when \mathcal{X} is the space of image-label pairs, $\Pi_{\mathcal{X}}$ clips images’ pixel values to $[0, 1]$ and ensures labels are valid probability distributions.)

¹In principle, the adversary can also decide *which* samples to poison, but for simplicity we consider this “fixed” case.



Figure 8: Examples of poisoned images from Section 4.3.

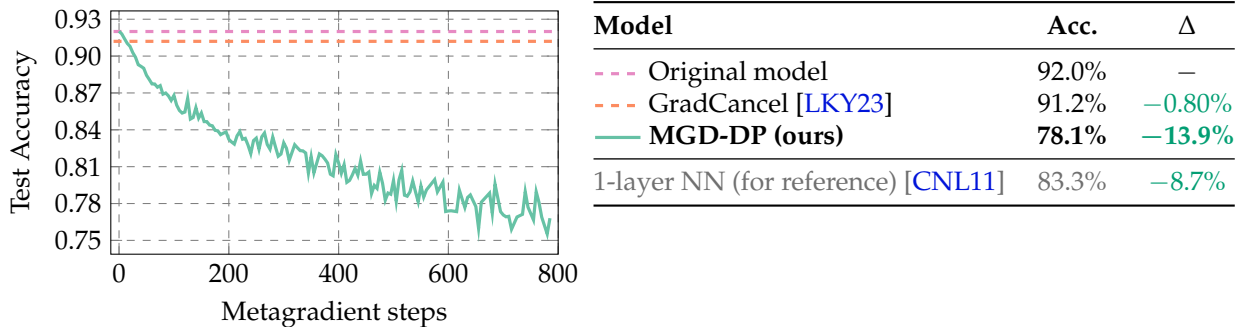


Figure 9: For each iteration of MGD (x -axis), we train a new model from random initialization on a randomly shuffled training set with the current iterate of poisoned data injected. We evaluate the test accuracy (y -axis), and use REPLAY to compute the metagradient. MGD outperforms the best known attack [LKY23] by an order of magnitude and (for reference) results in a model that has the same accuracy as a single-layer neural network trained on random image features [CNL11].

4.3.3 Evaluation

We use the CIFAR-10 dataset which consists of 60,000 total images each labeled as one of 10 classes. We partition the data into 40,000 training examples, 10,000 validation examples, and 10,000 test examples. We consider a simple 12-epoch CIFAR-10 training procedure, which reaches 92.4% accuracy on the CIFAR-10 test set when applied to the 40,000 training examples. See Appendix E for training hyperparameters.

As described above, we allow the adversary to modify (in-place) a fixed, ϵ -fraction of the training data (in our case, 2.5%) subject to the constraint that the poisoned images still lay in the valid (normalized) image range of $[0, 1]$. We compare our approach—direct optimization of the data poisoning objective using metagradients—to the state-of-the-art “Gradient Cancellation” (GradCancel) method of Lu et al. [LKY23]. In short, GradCancel is a two-step method which first finds a poorly performing model, then finds poisoned data that induces this model as a minimizer of the training loss. We present the full method in Appendix E.

Results. We find that metagradients enable state-of-the-art data poisoning attacks, degrading accuracy by 14%. In particular, when allowed to corrupt 1000 of the 40,000 training samples (2.5%), our method reduces test set accuracy to 78%—for reference, the accuracy of a single-layer neural network trained on the unmodified CIFAR-10 training set is 83%. The strongest existing data poisoning attack, GradCancel, only reduces test set accuracy by less than 1%.² In Figure 8, we visualize the poisoned images and labels found by our method. In Figure 9, we visualize the minibatch loss at each step of the optimization process.

Remark 4 (Poisoning non-smooth learning algorithms). *Recall that to apply metagradient descent, we alter the learning algorithm \mathcal{A} to be metasmooth (see Section 3.1). This involves making modifications such as switching out max pooling layers for average pooling layers, moving batch normalization layers before activations, and scaling down the last layer’s output by a factor of 10. It is natural to ask: how much does the efficacy of our method depend on this smoothness? After all, in practice the adversary cannot control the learning algorithm. To answer this question, we take the poison samples generated by MGD and insert them into the training set of a corresponding standard (i.e., non-metasmooth) learning algorithm. We find that our method still significantly degrades the performance of the model, from 92.8% to 82.6% (a drop of 10.2%).*

²Lu et al. [LKY23] report a larger drop; the discrepancy is due to our constraint that poisoned data are valid bounded RGB images.

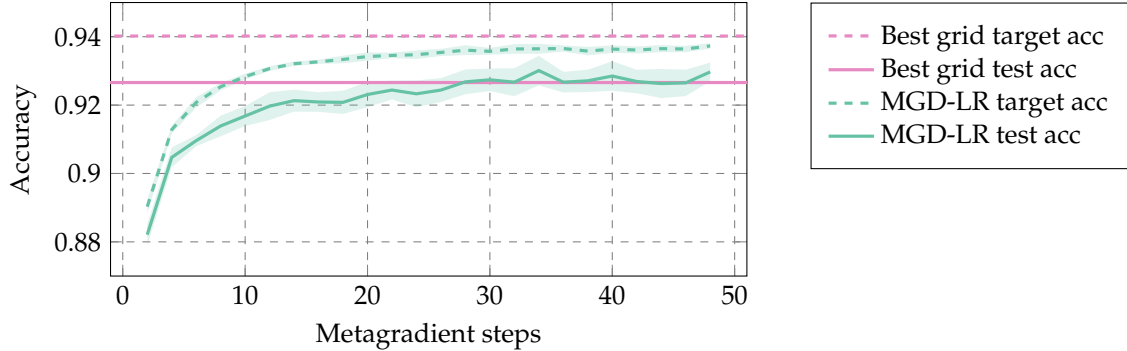


Figure 10: Target and test accuracies of MGD’s learning rate schedule over time closely match or exceed those found by a grid search over hundreds of combinations of hyperparameters. 95% confidence intervals are plotted for MGD’s results.

4.4 Finding a learning rate schedule

As a final application, we optimize the learning rate schedule of stochastic gradient descent (SGD) for training a CIFAR-10 classifier. By following the metagradients with respect to the learning rate at each step of training, our procedure matches grid searching over standard learning rate schedules—despite starting with naïve hyperparameters (a flat learning rate).

Unlike the other applications discussed here, metagradients do not unlock state-of-the-art performance. Instead, we discuss this application to illustrate the flexibility of REPLAY, and in particular its ability to optimize metaparameters that do not directly affect the loss landscape (i.e., that only affect the model via the optimization trajectory). As we discuss in Section 6, approximate metagradient estimators cannot apply to these metaparameters.

4.4.1 Setting

To put learning rate schedule optimization into the metagradient framework, we parameterize a schedule as a vector $\boldsymbol{\eta} \in \mathbb{R}^k$ comprising k evenly-spaced keypoints, so that the learning rate at iteration t is given by

$$\eta(t) = \eta_{\lfloor kt/T \rfloor} + \frac{kt/T - \lfloor kt/T \rfloor}{\lceil kt/T \rceil - \lfloor kt/T \rfloor} (\eta_{\lceil kt/T \rceil} - \eta_{\lfloor kt/T \rfloor}), \quad (10)$$

i.e., a linear interpolation between the keypoints.

- (a) the metaparameter $\boldsymbol{\eta} \in \mathbb{R}^k$ is a vector of k keypoints;
- (b) the algorithm \mathcal{A} maps metaparameters $\boldsymbol{\eta}$ to a trained model $\mathcal{A}(\boldsymbol{\eta})$ by training a model for T iterations with the learning rate schedule defined by (10);
- (c) the output function ϕ evaluates average loss on the validation set \mathbf{X}_{val} .

4.4.2 Algorithm

Following the theme of the rest of this section, we optimize the metaparameter $\boldsymbol{\eta}$ directly using MGD. In particular, we initialize the keypoints to be a flat learning rate schedule, and then update the keypoints using the metagradient with respect to the validation loss,

$$\boldsymbol{\eta}^{(t+1)} = \boldsymbol{\eta}^{(t)} - \alpha \cdot \text{sign} \left(\nabla_{\boldsymbol{\eta}} \phi(\mathcal{A}(\boldsymbol{\eta}^{(t)})) \right).$$

4.4.3 Evaluation

We aim to select the learning rate schedule that minimizes the expected test set loss. To do so, we reserve 90% of the CIFAR-10 test set as a “validation set” on which we select hyperparameters. We then use the remaining 10% as a test set. We compare the following two approaches:

- **Grid search:** We construct a grid over different one cycle learning rate schedules, varying the peak learning rate, starting learning rate, ending learning rate, and peak learning rate time. In total, we consider over 1,000 different learning rate schedules. We use the reserved 90% of the test set to select the best learning rate schedule from the grid.
- **Metagradient descent (MGD):** We run 50 steps of MGD starting from a highly suboptimal flat learning rate schedule, aiming to minimize loss on the reserved 90% of the test set. We use the last iteration of MGD as our learned learning rate schedule.

We evaluate the performance of each final learning rate schedule on the held-out 10% test set and average the results over the same set of 5 unseen random seeds.

Results. Comparing our learned hyperparameter schedule to grid search, as shown in Figure 10, our learned schedule using only 50 steps of MGD matches the performance of the state-of-the-art onecycle schedule found via grid search over more than 1000 configurations. An important caveat, however, is that these numbers are not directly comparable: grid search can be run in parallel across many machines, while steps of MGD must be run sequentially.

In practice, we do not advise using MGD for optimizing low-dimensional hyperparameters, especially ones that have been thoroughly optimized by grid search (such as CIFAR-10 learning rate schedules [SN17; Pag18; LA19; Jor24]). Still, an interesting avenue for future work is to study the utility of MGD for optimizing high-dimensional hyperparameters that are less well-studied, such as per-parameter/layer learning rates/weight decays for language models, attention hyperparameters, or gradient preconditioners.

5 Discussion

In this section, we first present the main limitations of our method and outline future directions.

Limitations. Although REPLAY is more efficient than existing methods at computing metagradients, it is still non-trivially more expensive than simply training a model once. The main reason is that metagradients require making a *backwards pass over a backwards pass*. This operation necessarily requires 2-3 times the operations of a backwards pass; furthermore, our current implementation requires `float32/tensorfloat32` operations. Finally, standard training operations are often made more efficient by specialized software (e.g., via FlashAttention [DFE+22]); no such software (yet) exists for backwards-over-backwards operations. Beyond computational issues, successfully applying metagradients requires smooth model training.

Metasmoothness: connections and future directions. While Section 3 describes a general procedure for finding metasmooth learning algorithms, an important future direction is to further explore and understand metasmoothness. This includes, for example: (a) characterizing the relationship between metasmoothness and numerical stability (and potentially using techniques from the latter to improve the former); (b) devising improved optimizers and/or architectures that lead directly to metasmooth learning algorithms (akin to skip connections or stable initialization in architecture design); (c) formalizing connections between metasmoothness and other optimization-related phenomena in deep learning [LM20; CKL+22]. A related but separate direction is to explore the possibility of using techniques from non-smooth optimization [Cla90] to perform metagradient descent on non-metasmooth learning algorithms.

Applying metagradients. Our methods apply to any ML task that requires optimizing with respect to a metaparameter. These include: poisoning data (generated or simply hosted on the internet) so that it cannot be trained on without permission (i.e., by maximizing training loss with respect to the text); selecting better training data at various stages of the model training lifecycle; and designing better model training routines and architectures with first-order methods. Another direction of future work lies in mitigating the computational limitations of our algorithm. Both (a) small-scale proxy-models [HBM+22; EFM24] and (b) low-hanging engineering improvements can likely make calculating metagradients much more efficient.

6 Related work

We overview previous work on calculating and applying meta-gradients.

6.1 Calculating metagradients

Previous work estimates the metagradient for large-scale models via one of two broad families of methods: implicit differentiation and automatic (explicit) differentiation. Note that in previous literature, synonyms for metagradient include “hyper-gradient” and “outer gradient.”

Implicit differentiation. One family of methods aims to *approximate* the metagradient. To illustrate the idea behind such approaches, suppose that the learning algorithm \mathcal{A} returns a model state θ that minimizes a strongly convex loss function $\mathcal{L}(z, \theta)$. Here, the implicit function theorem tells us that

$$\nabla_z f(z) = \overbrace{\left(\frac{d\phi}{d\theta} \Big|_{\theta=\mathcal{A}(z)} \right)}^{1 \times p \text{ gradient of output wrt. final params}} \underbrace{\left(\frac{\partial^2 \mathcal{L}(z, \theta)}{\partial \theta^2} \Big|_{\theta=\mathcal{A}(z)} \right)^{-1}}_{p \times p \text{ inverse Hessian of loss wrt. final params}} \overbrace{\left(\frac{\partial^2 \mathcal{L}(z, \theta)}{\partial \theta \partial z} \Big|_{\theta=\mathcal{A}(z)} \right)}^{p \times n \text{ Jacobian of loss gradient wrt. metaparameters}}. \quad (11)$$

The form of (11) yields efficient and accurate estimators for metagradients of models learned by minimizing a strongly convex loss [BKB+20; BKM+22; KDJ20; BBC+22; SGB+22]. Such approaches can extend to estimate metagradients of large-scale, non-convex learning algorithms [Ben00; KL17; RFK+19; FAL17; LVD20; CH20; BNL+22], but lose any correctness guarantees. Indeed, applying this class of methods in large-scale settings is challenging as doing so requires (a) assuming conditions on the learning algorithm (e.g., Hessian invertibility, continuous differentiability) and (b) efficiently approximating the inverse Hessian (in practice, typically at the cost of estimate accuracy). Finally, implicit function-based approaches are fundamentally limited in that they can only differentiate with respect to metaparameters expressed in the loss function (e.g., these methods can differentiate with respect to the weight decay, but not learning rate).

Automatic (explicit) differentiation. Beyond implicit differentiation approaches, there is a long line of work on directly calculating metagradients with AD (see Section 2). Previous work has used AD to estimate metagradients of learning algorithms ranging from those with convex objectives to small neural networks [HNM19; MDA15; FDF+17; MS21; ZSP+21; CXR+22; SGB+22]. As detailed in Section 2, the primary challenge with (reverse-mode) AD-based approaches to meta-differentiation is storing the intermediate products required for the backward pass. To circumvent this challenge, previous work either (a) only considers settings that are small enough that it is possible to differentiate while requiring space that is linear in the number of iterations (i.e., 2 layer networks on MNIST), (b) uses forward-mode AD [FDF+17; MS21; CXR+22] (which requires no extra storage at the cost of additional compute that scales linearly with metaparameter dimension), (c) only *approximates* the metagradient by calculating over only a few training steps [LSY18; CH20; FAL17], or uses (d) a reversible learning algorithm [MDA15]. The fourth category is a promising direction for reducing space requirements when computing large-scale metagradients, but current approaches require (a) representing model parameters in a fixed-precision format (which current large-scale learning algorithms do not support) in addition to restricting the algorithm to be reversible (e.g.,

SGD and standard GD do not qualify). A common thread is that algorithms computing metagradients with AD often suffer from numerical instability and overflow issues [MS21; SGB+22]. In relation to previous work on AD, REPLAY (Section 2) can be seen as a strategy for choosing gradient checkpointing [CAC+81; BCT92; ZP00; GW08; CXZ+16] locations in the compute graph (an NP-complete task in general [Nau08]).

6.2 Applying metagradients

Previous work applies metagradients to optimize training setup, including distillation [MDA15; LVD20], training data selection [HNM19; EFM24], meta-learning [FAL17; RFK+19; HAM+21], learning rate/weight decay selection [MS21; CXR+22], tuning data augmentation [LVD20], and architecture search [MDA15; LSY18; ZSP+21]. Beyond optimizing metagradients, methods in data attribution apply metagradients to (Taylor) estimate the effect of dropping training data on model predictions [KL17; GBA+23; PGI+23]. To the Previous works either (a) calculate metagradients directly with AD (made feasible by working in a very small-scale learning setting) or (b) estimate the metagradient with an implicit function-based approach.

7 Conclusion

In this work we add metagradients to the large-scale machine learning toolkit. To do so, we overcome two challenges: (a) calculating metagradients at scale and (b) modifying learning algorithms to be metasmooth—i.e., to admit metagradients that locally predict model behavior. We then successfully calculate and apply metagradients for large-scale models (up to 2B parameters) to select data for CLIP pretraining and instruction fine-tuning, to (Huber) poison training data to decrease overall model accuracy, and search for high-dimensional hyperparameters (per-iteration learning rates). Given the successful applications of metagradients in these settings, we are excited to see what unlocking metagradients enables in other areas of machine learning.

8 Acknowledgements

Work supported in part by the NSF grant DMS-2134108 and Open Philanthropy, and in part by NSF Grant No. 2346519. This work is also supported in part by the Alan Turing Institute, and the U.S. Department of Energy. The authors would like to thank Alex Damian, Harshay Shah, Jesse Michel, Joel Flynn, Manolis Zampetakis, Noah Moroze, Piotr Indyk, Sam Hopkins, Sung Min (Sam) Park, and Sarah Cen for helpful references as well as discussions and feedback on early versions of this work.

References

- [ATS+23] Amro Abbas, Kushal Tirumala, Dániel Simig, Surya Ganguli, and Ari S Morcos. “SemDeDup: Data-efficient learning at web-scale through semantic deduplication”. In: *arXiv preprint arXiv:2303.09540* (2023).
- [BAC+21] Sara Beery, Arushi Agarwal, Elijah Cole, and Vighnesh Birodkar. “The iWildCam 2021 competition dataset”. In: *arXiv preprint arXiv:2105.03494*. 2021.
- [BBC+22] Mathieu Blondel, Quentin Berthet, Marco Cuturi, Roy Frostig, Stephan Hoyer, Felipe Llinares-López, Fabian Pedregosa, and Jean-Philippe Vert. “Efficient and modular implicit differentiation”. In: *Advances in neural information processing systems* 35 (2022), pp. 5230–5242.
- [BBY+22] Yonatan Bitton, Nitzan Bitton Guetta, Ron Yosef, Yuval Elovici, Mohit Bansal, Gabriel Stanovsky, and Roy Schwartz. “WinoGAViL: Gamified association benchmark to challenge vision-and-language models”. In: *Advances in Neural Information Processing Systems*. 2022.
- [BCT92] Preston Briggs, Keith D Cooper, and Linda Torczon. “Rematerialization”. In: *Proceedings of the ACM SIGPLAN 1992 conference on Programming language design and implementation*. 1992, pp. 311–321.
- [Ben00] Yoshua Bengio. “Gradient-based optimization of hyperparameters”. In: *Neural computation* 12.8 (2000), pp. 1889–1900.
- [BGM+18] Peter Bandi, Oscar Geessink, Quirine Manson, Marcory Van Dijk, Maschenka Balkenhol, Meyke Hermsen, Babak Ehteshami Bejnordi, Byungjae Lee, Kyunghyun Paeng, Aoxiao Zhong, et al. “From detection of individual metastases to classification of lymph node status at the patient level: the CAMELYON17 challenge”. In: *IEEE Transactions on Medical Imaging* (2018).
- [BGV14] Lukas Bossard, Matthieu Guillaumin, and Luc Van Gool. “Food-101—mining discriminative components with random forests”. In: *European conference on computer vision*. 2014.
- [BKB+20] Quentin Bertrand, Quentin Klopfenstein, Mathieu Blondel, Samuel Vaiter, Alexandre Gramfort, and Joseph Salmon. “Implicit differentiation of lasso-type models for hyperparameter optimization”. In: *International Conference on Machine Learning*. PMLR. 2020, pp. 810–821.
- [BKM+22] Quentin Bertrand, Quentin Klopfenstein, Mathurin Massias, Mathieu Blondel, Samuel Vaiter, Alexandre Gramfort, and Joseph Salmon. “Implicit differentiation for fast hyperparameter selection in non-smooth convex learning”. In: *Journal of Machine Learning Research* 23.149 (2022), pp. 1–43.
- [BMA+19] Andrei Barbu, David Mayo, Julian Alverio, William Luo, Christopher Wang, Dan Gutfreund, Josh Tenenbaum, and Boris Katz. “ObjectNet: A large-scale bias-controlled dataset for pushing the limits of object recognition models”. In: *Neural Information Processing Systems (NeurIPS)*. 2019.
- [BNL+22] Juhan Bae, Nathan Ng, Alston Lo, Marzyeh Ghassemi, and Roger Grosse. “If Influence Functions are the Answer, Then What is the Question?”. In: *ArXiv preprint arXiv:2209.05364*. 2022.
- [BSF94] Yoshua Bengio, Patrice Simard, and Paolo Frasconi. “Learning long-term dependencies with gradient descent is difficult”. In: *IEEE Transactions on Neural Networks*. 1994.
- [CAC+81] Gregory J Chaitin, Marc A Auslander, Ashok K Chandra, John Cocke, Martin E Hopkins, and Peter W Markstein. “Register allocation via coloring”. In: *Computer languages* 6.1 (1981), pp. 47–57.
- [CFW+18] Gordon Christie, Neil Fendley, James Wilson, and Ryan Mukherjee. “Functional Map of the World”. In: *Proceedings of the IEEE Conference on Computer Vision and Pattern Recognition (CVPR)*. June 2018.
- [CH20] Xiangning Chen and Cho-Jui Hsieh. “Stabilizing differentiable architecture search via perturbation-based regularization”. In: *International conference on machine learning*. PMLR. 2020, pp. 1554–1565.

- [CHL17] Gong Cheng, Junwei Han, and Xiaoqiang Lu. “Remote sensing image scene classification: Benchmark and state of the art”. In: *Proceedings of the IEEE*. 2017.
- [CHM+23] Mike Conover, Matt Hayes, Ankit Mathur, Jianwei Xie, Jun Wan, Sam Shah, Ali Ghodsi, Patrick Wendell, Matei Zaharia, and Reynold Xin. *Free Dolly: Introducing the World’s First Truly Open Instruction-Tuned LLM*. 2023. URL: <https://www.databricks.com/blog/2023/04/12/dolly-first-open-commercially-viable-instruction-tuned-llm> (visited on 06/30/2023).
- [CKL+22] Jeremy M. Cohen, Simran Kaur, Yuanzhi Li, J. Zico Kolter, and Ameet Talwalkar. *Gradient Descent on Neural Networks Typically Occurs at the Edge of Stability*. 2022. arXiv: 2103.00065 [cs.LG]. URL: <https://arxiv.org/abs/2103.00065>.
- [Cla90] Frank H Clarke. *Optimization and nonsmooth analysis*. SIAM, 1990.
- [CMK+14] Mircea Cimpoi, Subhansu Maji, Iasonas Kokkinos, Sammy Mohamed, and Andrea Vedaldi. “Describing textures in the wild”. In: *Proceedings of the IEEE Conference on Computer Vision and Pattern Recognition*. 2014.
- [CNL11] Adam Coates, Andrew Ng, and Honglak Lee. “An analysis of single-layer networks in unsupervised feature learning”. In: *Proceedings of the fourteenth international conference on artificial intelligence and statistics*. 2011.
- [CXR+22] Kartik Chandra, Audrey Xie, Jonathan Ragan-Kelley, and Erik Meijer. “Gradient descent: The ultimate optimizer”. In: *Advances in Neural Information Processing Systems* 35 (2022), pp. 8214–8225.
- [CXZ+16] Tianqi Chen, Bing Xu, Chiyuan Zhang, and Carlos Guestrin. “Training Deep Nets with Sublinear Memory Cost”. In: *CoRR* abs/1604.06174 (2016). arXiv: 1604.06174. URL: <http://arxiv.org/abs/1604.06174>.
- [DDS+09] Jia Deng, Wei Dong, Richard Socher, Li-Jia Li, Kai Li, and Li Fei-Fei. “Imagenet: A large-scale hierarchical image database”. In: *Computer Vision and Pattern Recognition (CVPR)*. 2009.
- [DFE+22] Tri Dao, Daniel Y. Fu, Stefano Ermon, Atri Rudra, and Christopher Ré. *FlashAttention: Fast and Memory-Efficient Exact Attention with IO-Awareness*. 2022. arXiv: 2205.14135 [cs.LG]. URL: <https://arxiv.org/abs/2205.14135>.
- [DJP+24] Abhimanyu Dubey, Abhinav Jauhri, Abhinav Pandey, Abhishek Kadian, Ahmad Al-Dahle, Aiesha Letman, Akhil Mathur, Alan Schelten, Amy Yang, Angela Fan, et al. “The llama 3 herd of models”. In: *arXiv preprint arXiv:2407.21783* (2024).
- [Eco24] Team EcoDatum. *EcoDatum DataComp-small submission*. <https://www.datacomp.ai/dcclip/leaderboard.html>. 2024.
- [EFM24] Logan Engstrom, Axel Feldmann, and Aleksander Madry. “DsDm: Model-Aware Dataset Selection with Datamodels”. In: 2024.
- [EVW+10] M. Everingham, L. Van Gool, C. K. I. Williams, J. Winn, and A. Zisserman. “The Pascal Visual Object Classes (VOC) Challenge”. In: *International Journal of Computer Vision*. 2010.
- [FAL17] Chelsea Finn, Pieter Abbeel, and Sergey Levine. “Model-agnostic meta-learning for fast adaptation of deep networks”. In: *International conference on machine learning*. PMLR. 2017, pp. 1126–1135.
- [FDF+17] Luca Franceschi, Michele Donini, Paolo Frasconi, and Massimiliano Pontil. “Forward and reverse gradient-based hyperparameter optimization”. In: *International Conference on Machine Learning (ICML)*. 2017.
- [FFP04] Li Fei-Fei, Rob Fergus, and Pietro Perona. “Learning generative visual models from few training examples: An incremental bayesian approach tested on 101 object categories”. In: *2004 conference on computer vision and pattern recognition workshop*. IEEE. 2004, pp. 178–178.
- [FIW+22] Alex Fang, Gabriel Ilharco, Mitchell Wortsman, Yuhao Wan, Vaishaal Shankar, Achal Dave, and Ludwig Schmidt. “Data Determines Distributional Robustness in Contrastive Language Image Pre-training (CLIP)”. In: *ICML*. 2022.

- [GBA+23] Roger Grosse, Juhan Bae, Cem Anil, Nelson Elhage, Alex Tamkin, Amirhossein Tajdini, Benoit Steiner, Dustin Li, Esin Durmus, Ethan Perez, et al. “Studying large language model generalization with influence functions”. In: *arXiv preprint arXiv:2308.03296* (2023).
- [GDG17] Tianyu Gu, Brendan Dolan-Gavitt, and Siddharth Garg. “Badnets: Identifying Vulnerabilities in the Machine Learning Model Supply Chain”. In: *arXiv preprint arXiv:1708.06733* (2017).
- [GIF+24] Samir Yitzhak Gadre, Gabriel Ilharco, Alex Fang, Jonathan Hayase, Georgios Smyrnis, Thao Nguyen, Ryan Marten, Mitchell Wortsman, Dhruva Ghosh, Jieyu Zhang, et al. “DataComp: In search of the next generation of multimodal datasets”. In: *Advances in Neural Information Processing Systems*. 2024.
- [GLU12] Andreas Geiger, Philip Lenz, and Raquel Urtasun. “Are we ready for autonomous driving? The KITTI vision benchmark suite”. In: *2012 IEEE conference on computer vision and pattern recognition*. 2012.
- [GW08] Andreas Griewank and Andrea Walther. *Evaluating derivatives: principles and techniques of algorithmic differentiation*. SIAM, 2008.
- [HAM+21] Timothy Hospedales, Antreas Antoniou, Paul Micaelli, and Amos Storkey. “Meta-learning in neural networks: A survey”. In: *IEEE transactions on pattern analysis and machine intelligence* 44.9 (2021), pp. 5149–5169.
- [HBB+20] Dan Hendrycks, Collin Burns, Steven Basart, Andy Zou, Mantas Mazeika, Dawn Song, and Jacob Steinhardt. “Measuring massive multitask language understanding”. In: *arXiv preprint arXiv:2009.03300* (2020).
- [HBD+19] Patrick Helber, Benjamin Bischke, Andreas Dengel, and Damian Borth. “EuroSAT: A novel dataset and deep learning benchmark for land use and land cover classification”. In: *IEEE Journal of Selected Topics in Applied Earth Observations and Remote Sensing*. 2019.
- [HBK+21] Dan Hendrycks, Collin Burns, Saurav Kadavath, Akul Arora, Steven Basart, Eric Tang, Dawn Song, and Jacob Steinhardt. “Measuring Mathematical Problem Solving With the MATH Dataset”. In: *NeurIPS* (2021).
- [HBM+20] Dan Hendrycks, Steven Basart, Norman Mu, Saurav Kadavath, Frank Wang, Evan Dorundo, Rahul Desai, Tyler Zhu, Samyak Parajuli, Mike Guo, Dawn Song, Jacob Steinhardt, and Justin Gilmer. *The Many Faces of Robustness: A Critical Analysis of Out-of-Distribution Generalization*. 2020. arXiv: [2006.16241](https://arxiv.org/abs/2006.16241) [cs.CV].
- [HBM+22] Jordan Hoffmann, Sebastian Borgeaud, Arthur Mensch, Elena Buchatskaya, Trevor Cai, Eliza Rutherford, Diego de Las Casas, Lisa Anne Hendricks, Johannes Welbl, Aidan Clark, et al. “Training compute-optimal large language models”. In: *arXiv preprint arXiv:2203.15556*. 2022.
- [HNM19] Satoshi Hara, Atsushi Nitanda, and Takanori Maehara. “Data cleansing for models trained with SGD”. In: *Advances in Neural Information Processing Systems* 32 (2019).
- [Hub64] Peter J. Huber. “Robust estimation of a location parameter”. In: *The Annals of Mathematical Statistics*. 1964.
- [HY20] Jiaoyang Huang and Horng-Tzer Yau. “Dynamics of Deep Neural Networks and Neural Tangent Hierarchy”. In: *Proceedings of the 37th International Conference on Machine Learning*. 2020.
- [HZB+19] Dan Hendrycks, Kevin Zhao, Steven Basart, Jacob Steinhardt, and Dawn Song. “Natural adversarial examples”. In: *arXiv preprint arXiv:1907.07174* (2019).
- [JHV+17] Justin Johnson, Bharath Hariharan, Laurens Van Der Maaten, Li Fei-Fei, C Lawrence Zitnick, and Ross Girshick. “CLEVR: A diagnostic dataset for compositional language and elementary visual reasoning”. In: *Proceedings of the IEEE conference on computer vision and pattern recognition*. 2017.
- [Jor24] Keller Jordan. “94 percent on CIFAR-10 in 3.29 Seconds on a Single GPU”. In: (2024).
- [JS08] Yaochu Jin and Bernhard Sendhoff. “Pareto-based multiobjective machine learning: An overview and case studies”. In: *IEEE Transactions on Systems, Man, and Cybernetics, Part C (Applications and Reviews)* 38.3 (2008), pp. 397–415.

- [KB15] Diederik P. Kingma and Jimmy Ba. “Adam: A Method for Stochastic Optimization”. In: *International Conference on Learning Representations (ICLR)*. 2015.
- [KDJ20] MJ Zico Kolter, David Duvenaud, and Matt Johnson. “Deep implicit layers-neural odes, deep equilibrium models, and beyond, 2020”. In: *NeurIPS Tutorial* (2020).
- [KKR+24] Andreas Köpf, Yannic Kilcher, Dimitri von Rütte, Sotiris Anagnostidis, Zhi Rui Tam, Keith Stevens, Abdullah Barhoum, Duc Nguyen, Oliver Stanley, Richárd Nagyfi, et al. “Openassistant conversations-democratizing large language model alignment”. In: *Advances in Neural Information Processing Systems* 36 (2024).
- [KL17] Pang Wei Koh and Percy Liang. “Understanding Black-box Predictions via Influence Functions”. In: *International Conference on Machine Learning*. 2017.
- [Kri09] Alex Krizhevsky. “Learning Multiple Layers of Features from Tiny Images”. In: *Technical report*. 2009.
- [KSD+13] Jonathan Krause, Michael Stark, Jia Deng, and Li Fei-Fei. “3d object representations for fine-grained categorization”. In: *Proceedings of the IEEE international conference on computer vision workshops*. 2013.
- [KSM+20] Pang Wei Koh, Shiori Sagawa, Henrik Marklund, Sang Michael Xie, Marvin Zhang, Akshay Balsubramani, Weihua Hu, Michihiro Yasunaga, Richard Lanus Phillips, Sara Beery, et al. “WILDS: A Benchmark of in-the-Wild Distribution Shifts”. In: *arXiv preprint arXiv:2012.07421* (2020).
- [LA19] Zhiyuan Li and Sanjeev Arora. *An Exponential Learning Rate Schedule for Deep Learning*. 2019.
- [LeC98] Yann LeCun. “The MNIST database of handwritten digits”. In: *Technical report*. 1998.
- [LFX+24] Aixin Liu, Bei Feng, Bing Xue, Bingxuan Wang, Bochao Wu, Chengda Lu, Chenggang Zhao, Chengqi Deng, Chenyu Zhang, Chong Ruan, et al. “Deepseek-v3 technical report”. In: *arXiv preprint arXiv:2412.19437*. 2024.
- [LHV+23] Shayne Longpre, Le Hou, Tu Vu, Albert Webson, Hyung Won Chung, Yi Tay, Denny Zhou, Quoc V Le, Barret Zoph, Jason Wei, et al. “The flan collection: Designing data and methods for effective instruction tuning”. In: *International Conference on Machine Learning*. PMLR. 2023, pp. 22631–22648.
- [LIE+22] Guillaume Leclerc, Andrew Ilyas, Logan Engstrom, Sung Min Park, Hadi Salman, and Aleksander Madry. *ffcv*. <https://github.com/libffcv/ffcv/>. 2022.
- [LKY22] Yiwei Lu, Gautam Kamath, and Yaoliang Yu. “Indiscriminate Data Poisoning Attacks on Neural Networks”. In: *arXiv preprint arXiv:2204.09092* (2022).
- [LKY23] Yiwei Lu, Gautam Kamath, and Yaoliang Yu. “Exploring the limits of model-targeted indiscriminate data poisoning attacks”. In: *International Conference on Machine Learning*. PMLR. 2023, pp. 22856–22879.
- [LM20] Guillaume Leclerc and Aleksander Madry. “The two regimes of deep network training”. In: *arXiv preprint arXiv:2002.10376*. 2020.
- [LMB+14] Tsung-Yi Lin, Michael Maire, Serge Belongie, James Hays, Pietro Perona, Deva Ramanan, Piotr Dollár, and C Lawrence Zitnick. “Microsoft coco: Common objects in context”. In: *European conference on computer vision (ECCV)*. 2014.
- [LSY18] Hanxiao Liu, Karen Simonyan, and Yiming Yang. “Darts: Differentiable architecture search”. In: *arXiv preprint arXiv:1806.09055* (2018).
- [LVD20] Jonathan Lorraine, Paul Vicol, and David Duvenaud. “Optimizing millions of hyperparameters by implicit differentiation”. In: *International conference on artificial intelligence and statistics*. PMLR. 2020, pp. 1540–1552.
- [MDA15] Dougal Maclaurin, David Duvenaud, and Ryan Adams. “Gradient-based hyperparameter optimization through reversible learning”. In: *International conference on machine learning (ICML)*. 2015.

- [MRK+13] Subhransu Maji, Esa Rahtu, Juho Kannala, Matthew Blaschko, and Andrea Vedaldi. “Fine-grained visual classification of aircraft”. In: *arXiv preprint arXiv:1306.5151* (2013).
- [MS21] Paul Micaelli and Amos J Storkey. “Gradient-based hyperparameter optimization over long horizons”. In: *Advances in Neural Information Processing Systems* 34 (2021), pp. 10798–10809.
- [Nau08] Uwe Naumann. “Optimal Jacobian accumulation is NP-complete”. In: *Math. Program.* 112.2 (Apr. 2008), pp. 427–441. ISSN: 0025-5610.
- [NWC+11] Yuval Netzer, Tao Wang, Adam Coates, Alessandro Bissacco, Baolin Wu, Andrew Y Ng, et al. “Reading digits in natural images with unsupervised feature learning”. In: *NIPS workshop on deep learning and unsupervised feature learning*. 2011.
- [NZ08] Maria-Elena Nilsback and Andrew Zisserman. “Automated flower classification over a large number of classes”. In: *2008 Sixth Indian Conference on Computer Vision, Graphics & Image Processing*. 2008.
- [OR00] James M Ortega and Werner C Rheinboldt. *Iterative solution of nonlinear equations in several variables*. SIAM, 2000.
- [Pag18] David Page. *CIFAR-10 Fast*. GitHub Repository. Oct. 2018. URL: <https://github.com/davidcpage/cifar10-fast>.
- [Pea96] Barak A Pearlmutter. “An investigation of the gradient descent process in neural networks”. In: *PhD thesis, Carnegie Mellon University*. 1996.
- [PGI+23] Sung Min Park, Kristian Georgiev, Andrew Ilyas, Guillaume Leclerc, and Aleksander Madry. “TRAK: Attributing Model Behavior at Scale”. In: *Arxiv preprint arXiv:2303.14186*. 2023.
- [PVZ+12] Omkar M Parkhi, Andrea Vedaldi, Andrew Zisserman, and CV Jawahar. “Cats and dogs”. In: *2012 IEEE conference on computer vision and pattern recognition*. IEEE. 2012, pp. 3498–3505.
- [RDK+22] William A Gaviria Rojas, Sudnya Diamos, Keertan Ranjan Kini, David Kanter, Vijay Janapa Reddi, and Cody Coleman. “The dollar street dataset: Images representing the geographic and socioeconomic diversity of the world”. In: *Thirty-sixth Conference on Neural Information Processing Systems Datasets and Benchmarks Track*. 2022.
- [RFK+19] Aravind Rajeswaran, Chelsea Finn, Sham M Kakade, and Sergey Levine. “Meta-learning with implicit gradients”. In: *Advances in neural information processing systems* 32 (2019).
- [RKH+21] Alec Radford, Jong Wook Kim, Chris Hallacy, Aditya Ramesh, Gabriel Goh, Sandhini Agarwal, Girish Sastry, Amanda Askell, Pamela Mishkin, Jack Clark, et al. “Learning transferable visual models from natural language supervision”. In: *arXiv preprint arXiv:2103.00020*. 2021.
- [RLZ+24] Vikram V Ramaswamy, Sing Yu Lin, Dora Zhao, Aaron Adcock, Laurens van der Maaten, Deepti Ghadiyaram, and Olga Russakovsky. “GeoDE: a geographically diverse evaluation dataset for object recognition”. In: *Advances in Neural Information Processing Systems*. 2024.
- [RRS+19] Benjamin Recht, Rebecca Roelofs, Ludwig Schmidt, and Vaishaal Shankar. “Do ImageNet Classifiers Generalize to ImageNet?” In: *International Conference on Machine Learning (ICML)*. 2019.
- [SGB+22] Damien Scieur, Gauthier Gidel, Quentin Bertrand, and Fabian Pedregosa. “The curse of unrolling: Rate of differentiating through optimization”. In: *Advances in Neural Information Processing Systems* 35 (2022), pp. 17133–17145.
- [SN17] Leslie N. Smith Smith and Topin Nicholay. “Super-Convergence: Very Fast Training of Neural Networks Using Large Learning Rates”. In: *ArXiv preprint arXiv:1708.07120*. 2017.
- [SRR+22] Aarohi Srivastava, Abhinav Rastogi, Abhishek Rao, Abu Awal Md Shoeb, Abubakar Abid, Adam Fisch, Adam R Brown, Adam Santoro, Aditya Gupta, Adrià Garriga-Alonso, et al. “Beyond the imitation game: Quantifying and extrapolating the capabilities of language models”. In: *arXiv preprint arXiv:2206.04615* (2022).
- [SSS+11] Johannes Stalkamp, Marc Schlipf, Jan Salmen, and Christian Igel. “The German traffic sign recognition benchmark: a multi-class classification competition”. In: *The 2011 international joint conference on neural networks*. 2011.

- [SSS+22] Mirac Suzgun, Nathan Scales, Nathanael Schärli, Sebastian Gehrmann, Yi Tay, Hyung Won Chung, Aakanksha Chowdhery, Quoc V Le, Ed H Chi, Denny Zhou, et al. “Challenging big-bench tasks and whether chain-of-thought can solve them”. In: *arXiv preprint arXiv:2210.09261* (2022).
- [TGZ+23] Rohan Taori, Ishaan Gulrajani, Tianyi Zhang, Yann Dubois, Xuechen Li, Carlos Guestrin, Percy Liang, and Tatsunori B. Hashimoto. *Stanford Alpaca: An Instruction-following LLaMA model*. https://github.com/tatsu-lab/stanford_alpaca. 2023.
- [TMH+24] Gemma Team, Thomas Mesnard, Cassidy Hardin, Robert Dadashi, Surya Bhupatiraju, Shreya Pathak, Laurent Sifre, Morgane Rivière, Mihir Sanjay Kale, Juliette Love, et al. “Gemma: Open models based on gemini research and technology”. In: *arXiv preprint arXiv:2403.08295* (2024).
- [TSF+16] Bart Thomee, David A. Shamma, Gerald Friedland, Benjamin Elizalde, Karl Ni, Douglas Poland, Damian Borth, and Li-Jia Li. “YFCC100M: The New Data in Multimedia Research”. In: *Communications of the ACM* (2016).
- [VLW+18] Bastiaan S Veeling, Jasper Linmans, Jim Winkens, Taco Cohen, and Max Welling. “Rotation equivariant CNNs for digital pathology”. In: *Medical Image Computing and Computer Assisted Intervention—MICCAI 2018: 21st International Conference, Granada, Spain, September 16-20, 2018, Proceedings, Part II* 11. 2018.
- [Web24] Team Webdataset. *webdataset*. 2024. URL: <https://www.github.com/webdataset/webdataset>.
- [Wer90] Paul J Werbos. “Backpropagation through time: what it does and how to do it”. In: *Proceedings of the IEEE* 78.10 (1990), pp. 1550–1560.
- [WGX+19] Haohan Wang, Songwei Ge, Eric P Xing, and Zachary C Lipton. “Learning robust global representations by penalizing local predictive power”. In: *Neural Information Processing Systems (NeurIPS)* (2019).
- [WWS+22] Jason Wei, Xuezhi Wang, Dale Schuurmans, Maarten Bosma, Fei Xia, Ed Chi, Quoc V Le, Denny Zhou, et al. “Chain-of-thought prompting elicits reasoning in large language models”. In: *Advances in neural information processing systems* 35 (2022), pp. 24824–24837.
- [XHE+10] Jianxiong Xiao, James Hays, Krista A Ehinger, Aude Oliva, and Antonio Torralba. “Sun database: Large-scale scene recognition from abbey to zoo”. In: *Computer Vision and Pattern Recognition (CVPR)*. 2010.
- [XMG+24] Mengzhou Xia, Sadhika Malladi, Suchin Gururangan, Sanjeev Arora, and Danqi Chen. “Less: Selecting influential data for targeted instruction tuning”. In: *arXiv preprint arXiv:2402.04333* (2024).
- [YLH+14] Peter Young, Alice Lai, Micah Hodosh, and Julia Hockenmaier. “From image descriptions to visual denotations: New similarity metrics for semantic inference over event descriptions”. In: *Transactions of the Association for Computational Linguistics*. 2014.
- [ZP00] Geoffrey Zweig and Mukund Padmanabhan. “Exact alpha-beta computation in logarithmic space with application to MAP word graph construction”. In: *Sixth International Conference on Spoken Language Processing, ICSLP 2000 / INTERSPEECH 2000, Beijing, China, October 16-20, 2000*. ISCA, 2000, pp. 855–858. DOI: [10.21437/ICSLP.2000-404](https://doi.org/10.21437/ICSLP.2000-404). URL: <https://doi.org/10.21437/ICSLP.2000-404>.
- [ZPK+19] Xiaohua Zhai, Joan Puigcerver, Alexander Kolesnikov, Pierre Ruysen, Carlos Riquelme, Mario Lucic, Josip Djolonga, Andre Susano Pinto, Maxim Neumann, Alexey Dosovitskiy, et al. “A large-scale study of representation learning with the visual task adaptation benchmark”. In: *arXiv preprint arXiv:1910.04867*. 2019.
- [ZSP+21] Miao Zhang, Steven W Su, Shirui Pan, Xiaojun Chang, Ehsan M Abbasnejad, and Reza Haffari. “idarts: Differentiable architecture search with stochastic implicit gradients”. In: *International Conference on Machine Learning*. PMLR. 2021, pp. 12557–12566.

A Calculating metagradients with REPLAY

This appendix contains supplementary material for Section 2. We describe two algorithms in detail: step-wise AD, and our own algorithm REPLAY. Refer to Section 2 for the notation used in this appendix.

A.1 Warmup: Step-wise AD

We fully describe step-wise AD in Algorithm 2. The algorithm requires storing all T optimizer states, but requires constant memory overhead for each AD call (as each AD call is over a single step), making it feasible to compute for small setups.

Algorithm 2: metagradients in $\mathcal{O}(T)$ space.

```

1 // Store each optimizer state on disk
2  $\{s_i\}_{i=0}^T \leftarrow \text{Train model via } A(z)$ 
3
4 // Variables; shorthand for  $\frac{\partial f(z)}{\partial z}$  and  $\frac{\partial f(z)}{\partial s_T}$ 
5  $\bar{z} \leftarrow 0$ 
6  $\bar{s}_T \leftarrow \frac{\partial g(s_T)}{\partial s_T}$  // One reverse-mode AD call
7
8 // Reverse-mode differentiate step-by-step
9 for  $s_i \leftarrow s_{T-1}$  to  $s_0$  do
10 | // One reverse-mode AD call. Left:  $\nabla_{s_i} f$ . Right: contribution to  $\nabla_z f$  at  $i$ .
11 |  $\bar{s}_i \leftarrow \bar{s}_{i+1} \cdot \frac{\partial h_i(s_i, z)}{\partial s_i}$ ,  $\bar{z}_i \leftarrow \bar{s}_{i+1} \cdot \frac{\partial h_i(s_i, z)}{\partial z}$ 
12 |
13 |  $\bar{z} \leftarrow \bar{z} + \bar{z}_i$  // Accumulate metagradient
14
15 Return  $\bar{z}$ 

```

A.2 REPLAY

We now describe REPLAY, our method for calculating metagradients. For a free parameter $k \in \mathbb{N}$, REPLAY requires storing $\mathcal{O}(k \log_k(T))$ optimizer states and an additional $\mathcal{O}(\log_k(T))$ factor of computation. The free parameter k controls the trade-off between storage and required compute. We fully describe REPLAY in Algorithm 3. REPLAY modifies Algorithm 2 by retrieving the optimizer states in reverse order using a k -ary tree structure in lieu of a list of all the stored states.

A.2.1 Lazy k -ary tree

We now describe the k -ary tree structure that underlies REPLAY; for a visual reference of this tree with $k = 2$, see Figure 3. For ease of analysis we parameterize the total number of states as $n = T + 1$ (and therefore take $n - 1$ total training steps) when describing this data structure, and assume WLOG that n is an integer power of k . At a high level, traversing this tree recursively replays retraining to recover all the optimizer states in reverse order, while deleting states that are no longer needed. We call this tree “lazy” because it retrains only when required to obtain states that are not yet retrieved.

The tree is a complete k -ary tree with n leaves (and therefore $\log_k(n)$ depth) structured as follows. We start at the root, then recursively define the rest of the tree. Every node in the tree represents a single optimizer state. The root represents state s_0 . To recursively define the remaining nodes: each non-leaf node s_i at depth d has k equally spaced (in terms of state number) children starting—from left to right—at state s_i and ending at $s_{i+n/k^{d+1}}$. This means that the leaves correspond—from left to right—to the states s_0, s_1, \dots, s_{n-1} .

We reduce the problem of iterating over the states in reverse to the problem of reverse in-order traversing this tree and yielding *just* the leaves—this is exactly the states in reverse order. A reverse in-order traversal for this k -ary tree requires repeatedly: recursively traversing child nodes from largest to smallest, then visiting the parent node. We design the specifics of this traversal to maximize space and compute efficiency. To access the children of a parent node at traversal time, we replay model training from the smallest child state (which is stored in the parent state) to the largest child state and store all the children. We perform this operation recursively each time we traverse a node. After traversing the node’s left side (i.e., after ascending from this node), we delete all its child states.

Reverse in-order traversing this tree requires storing at most $k \log_k(n)$ optimizer states at a time, and in aggregate requires retraining the model $\log_k(n)$ times. The argument for each is straightforward. Storage: the traversal requires storing at most k states for each level that it descends (we store k states whenever we first traverse to a parent node) and we remove k states for each level that the traversal ascends (we remove k states after we are done with the left traversal of a parent). Compute: we replay training to reinitialize the children of every parent node a single time. The k^d parent nodes at level d each require replaying $\mathcal{O}(n/k^d)$ states to reinitialize children. Therefore, in a traversal, each level requires $\mathcal{O}(n)$ ($k^d \cdot n/k^d$) optimizer steps. There are $\log_k(n)$ levels with parent nodes, which means a total of $\mathcal{O}(n \log_k(n))$ optimizer steps, or a multiplicative factor of $\mathcal{O}(\log_k(n))$ steps compared to model training.

Algorithm 3: REPLAY. metagradients in $\mathcal{O}(k \log_k(T))$ space.

```

1  $T \leftarrow$  Lazy  $k$ -ary tree for  $\mathcal{A}(z)$  // Make lazy  $k$ -ary tree of Appendix A.2
2
3 // Variables; shorthand for  $\frac{\partial f(z)}{\partial z}$  and  $\frac{\partial f(z)}{\partial s_T}$ 
4  $\bar{z} \leftarrow 0$ 
5  $\bar{s}_T \leftarrow \frac{\partial g(s_T)}{\partial s_T}$  // One reverse-mode AD call
6
7 // Reverse-mode differentiate step-by-step; traverse  $T$  instead of stored states
8 for  $s_i \leftarrow s_{T-1}$  to  $s_0 \in$  reverse_inorder_traversal( $T$ ) do
9     // One reverse-mode AD call. Left:  $\nabla_{s_i} f$ . Right: contribution to  $\nabla_z f$  at  $i$ .
10     $\bar{s}_i \leftarrow \bar{s}_{i+1} \cdot \frac{\partial h_i(s_i, z)}{\partial s_i}$ ,  $\bar{z}_i \leftarrow \bar{s}_{i+1} \cdot \frac{\partial h_i(s_i, z)}{\partial z}$ 
11
12     $\bar{z} \leftarrow \bar{z} + \bar{z}_i$  // Accumulate metagradient
13
14 Return  $\bar{z}$ 

```

B Smooth Model Training

B.1 Omitted Figures

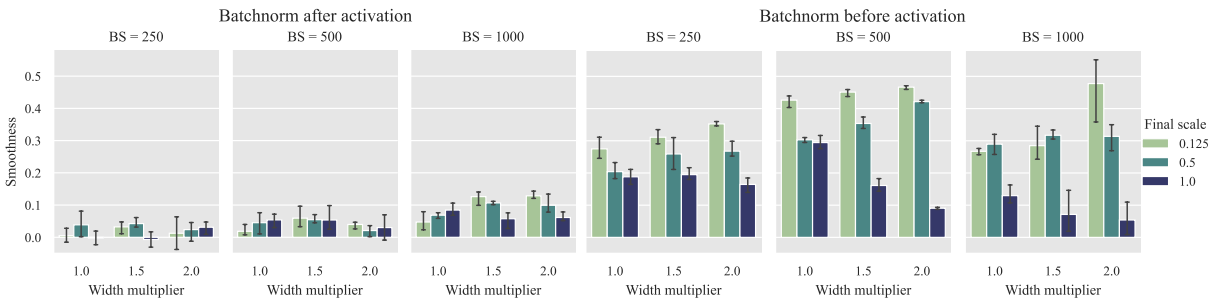


Figure 11: The factors affecting metasmoothness of training a ResNet-9 on the CIFAR-10 dataset. See §3 for details.

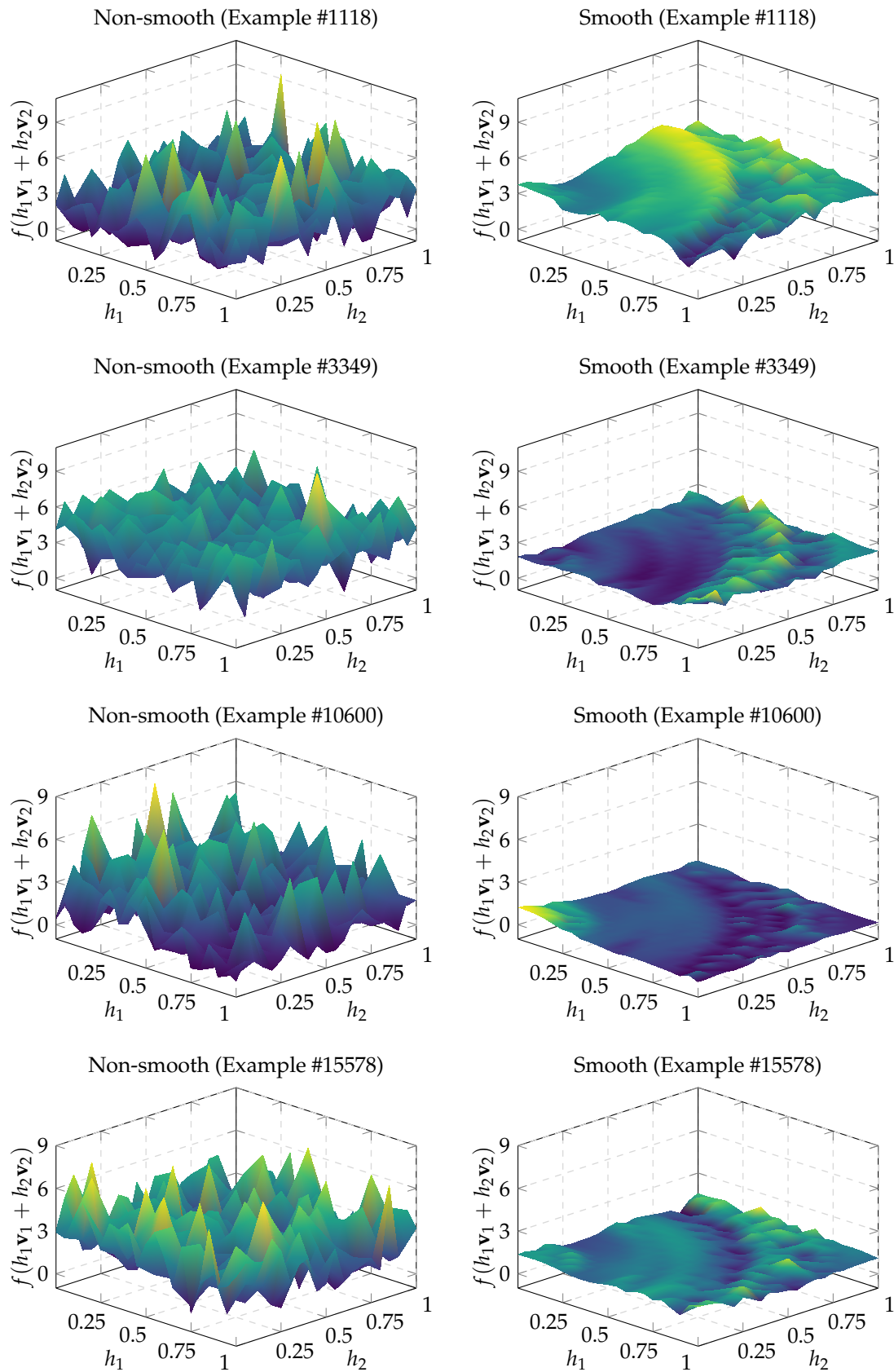


Figure 12: Additional loss landscape visualizations.

C Metagradients for DataComp

This appendix contains pseudocode for the main algorithm used to do dataset selection for DataComp. It also contains additional implementation details on how metagradients were applied to CLIP, and how they were specifically applied to the DataComp setting.

C.1 Dataset Selection Using MGD

When implementing Algorithm 1, there are several differences from the pseudocode below: firstly, rather than selecting \mathbf{m} fully randomly every step, we randomly select a shard comprising fraction p of the data and take steps on all datapoints in the shard (see Section C.2). To mitigate overfitting, we also bake a “minibatch fraction” q into our model output function ϕ . For example, if ϕ calculates model loss on the ImageNet train set, each time ϕ is called, we randomly sample fraction q of the ImageNet train set to evaluate on.

Adapting the CLIP loss function to our surrogate learning algorithm. Here, we explain how dataweights are incorporated into the CLIP loss function—the formulation given in Section 4.1 is actually slightly simplified and incorrect, as it does not account for cross terms in the CLIP contrastive loss. As a refresher, we first state the “vanilla” CLIP loss function, ℓ , as it is defined in [RKH+21]. Letting b be the batch size and d be the embedding dimension, and \mathbf{x} be the training batch at timestep k . Recall that the CLIP model internally has two “submodules”: and image embedder, and a text embedder. We then use these to obtain image embeddings $E_I \in \mathbb{R}^{b \times d}$ and text embeddings $E_T \in \mathbb{R}^{b \times d}$ from \mathbf{x} . We then compute the image-wise scores, or logits, for this batch as $S = E_I E_T^\top$ ³. Then, we can define the CLIP loss (as a function of the logits) as

$$L(S) = \frac{1}{2}(L_I(S) + L_T(S)),$$

where L_I and L_T are row-wise and column-wise cross-entropy losses, respectively:

$$L_I(S) = \sum_{i=1}^b \log \left(\frac{\exp(S_{i,i})}{\sum_{j=1}^b \exp(S_{i,j})} \right), \quad L_T(S) = \sum_{i=1}^b \log \left(\frac{\exp(S_{i,i})}{\sum_{j=1}^b \exp(S_{j,i})} \right).$$

We now wish to relax L into a new function L' that supports an additional input $\mathbf{z} \in \mathbb{R}^n$, where $\frac{\partial L'}{\partial \mathbf{z}}$ resembles the metagradients with respect to dataweights. In order to do this, we imagine expanding passing the *entire dataset* D into our embedder to obtain E'_I and E'_T , and take our new logits $S' = E'_I E'^\top_T \in \mathbb{R}^{n \times n}$.

There are some additional key conditions our relaxation L' should satisfy. Particularly: when $\mathbf{z} = \mathbf{0}_n$, we should recover the normal CLIP loss L , and when \mathbf{z} is all 0’s except for a single entry i , L' should act as if i had been appended to the original batch \mathbf{x} . In addition, L' should always have meaningful partials with respect to \mathbf{z} , even when some values in \mathbf{z} are 0.

Letting $\mathbf{1}_{i=j}$ and $\mathbf{1}_{i \neq j}$ be indicator variables and letting $\mathbf{1}_k \in \{0, 1\}^n$ be the indicator vector for the k -th batch, we find that the definition

$$L'(S', \mathbf{z}) = L'_I(S', \mathbf{z}) + L'_T(S', \mathbf{z}),$$

where

$$L'_I(S', \mathbf{z}) = \sum_{i=1}^n (z_i + (\mathbf{1}_k)_i) \log \left(\frac{\exp(S'_{i,i})}{\sum_{j=1}^n \exp(S'_{i,j}) (\mathbf{1}_{i=j} + \mathbf{1}_{i \neq j} (z_j + (\mathbf{1}_k)_j))} \right)$$

and

$$L'_T(S', \mathbf{z}) = \sum_{i=1}^n (z_i + (\mathbf{1}_k)_i) \log \left(\frac{\exp(S'_{i,i})}{\sum_{j=1}^n \exp(S'_{j,i}) (\mathbf{1}_{i=j} + \mathbf{1}_{i \neq j} (z_j + (\mathbf{1}_k)_j))} \right)$$

satisfy these conditions.

³The CLIP model scales these logits by a temperature parameter τ before applying the softmax. While we omit τ in our definitions, it can be easily incorporated. All our experiments use temperature scaling.

Finally, we let define the loss for the entire batch ℓ' as a function of \mathbf{z} and model parameters θ which outputs the loss calculated according to L' above. To summarize, letting $\mathbf{x}^{(t)}$ denote the t -th training batch, the loss function ℓ_t at step t of our surrogate learning algorithm \mathcal{A}' for CLIP training is:

$$\ell'_t(\theta) := \begin{cases} \ell(\mathbf{x}^{(t)}; \theta) & \text{if } t \neq k \\ \ell'(\mathbf{z}; \theta) & \text{if } t = k. \end{cases}$$

We find that this empirically works well for obtaining meaningful metagradients with respect to dataweights in the CLIP setting, and yields to strong dataset selection results.

C.2 Scaling MGD for CLIP and DataComp

MGD is highly scalable, allowing it to be applied to large-scale settings like training CLIP models. In particular, computing metagradients is only up to a constant factor more expensive than training a model normally. Here, we outline challenges we faced in scaling MGD in this setting, and how they were resolved. Specifically, we will explain how we efficiently calculated metagradients for CLIP models and efficiently tracked/shuffled our dataset selection from step-to-step despite its large storage footprint.

Computing metagradients. Due to the large batch size used in the CLIP contrastive loss, we implement manual gradient checkpointing to make the operations computationally feasible on our hardware. The most memory-intensive operation are model forward passes (and its gradients): obtaining the image and label embeddings given raw pixel data and tokens. So, we manually make gradient checkpoints before this operation, allowing us to run the embedder in minibatches to avoid memory issues. This setup also naturally lends itself to parallelization across multiple GPU’s, which we make use of to further speed up our computations.

Loading, writing, and storing data. Due to the data-intensive nature of training large models like CLIP and our need to frequently produce new datasets at each optimization step, we found that using the web-dataset [Web24] format given by DataComp was restrictively slow. To circumvent this, we rewrote all data following the format of FFCV [LIE+22], allowing us to load and write data much faster. Specifically, we divided the entire candidate pool into 8 base shards. Once we trained a model, we choose one of the 8 shards, compute metagradients corresponding to all datapoints in the shard, take a gradient step on them, and rewrite the shard. This roughly corresponds to $p = \frac{1}{8}$ in Algorithm 1, which we empirically worked well for optimizing. In following steps, we always choose one of the 8 *original* shards to calculate metagradients for—this ensures that points removed from the dataset in some optimization step can return if they have a negative metagradient.

We also observed that always stepping on the sign causes the sizes of the shards to grow over time: stepping based on the sign of the metagradient does not decrease the weight on a positive-weight datapoint if its dataweight is already 0, so our steps are biased towards increasing the size of the shards. To combat this blowup, after some number of optimization steps, we choose a fixed shard size and enforce that subsequent steps must not change the size of the shards—the step size thereafter is controlled by hyperparameter q representing the fraction of datapoints in a shard which are incremented. We experimented both with randomly sampling which points are added or removed, and stepping on the datapoints with the top q and bottom q metagradients; the latter seems to give empirically better performance.

To maintain randomness during shuffling, we implement an 8-way dataloader which would shuffle all 8 shards individually. Then, to sample a batch of b datapoints, we would sample $b/8$ datapoints from each shard and concatenate them to fill our batch. This works better than simply sampling our entire batch from a single shard, as (especially in later optimization steps) shards may contain a high number of duplicate datapoints, which causes CLIP’s contrastive loss function to misbehave if they appear in the same batch.

To minimize disk space used, old shards can be deleted once they become “stale”. Specifically, if shard s is rewritten into shard s' , all future optimization steps will never read s again, and s can safely be deleted. Thus, when running MGD for a large number of steps and potentially rewriting each shard multiple times, the total disk space used by our algorithm is constant in the number of steps we take: it stores the 8 most recently written shards on disk at any given time, and any other shards are deleted to save space.

C.3 Details Pertaining to the DataComp Benchmark

Setting. We provide a brief summary of the DataComp competition here, and we refer readers to the original paper [GIF+24]. DataComp is a framework to compare different training dataset selection techniques. Participants submit a training dataset (which, for our purposes, is a subset of a larger dataset), upon which a CLIP model is trained from scratch with a fixed learning algorithm, model architecture, and number of training steps. We focus on DataComp-small, which has a candidate pool of 12.8 million samples. The number of training steps in this case is also fixed at 12.8 million samples.

We try to match the optimization hyperparameters enforced by DataComp as closely as possible. As a refresher, our ADAM[KB15] update step can be written as

$$\theta_{t+1} = -\alpha_t \cdot (m_t / (\sqrt{v_t + \epsilon_{\text{root}} + \epsilon}) + \lambda\theta_t) \tag{12}$$

where m_t and v_t are running estimates of the first and second moments of the gradients, respectively, λ represents weight decay, α represents the learning rate, and ϵ and ϵ_{root} are hyperparameters to avoid blowup. Our training hyperparameters can be found in Table 1 and are identical to those mandated by DataComp-small, aside from a positive ϵ_{root} added for numerical stability. The values of ϵ_{root} and k (the step at which metagradients are calculated) were chosen to empirically maximize metasmoothness.

Table 1: Hyperparameters for the CLIP DataComp experiments.

Hyperparameter	Value
DataComp Scale	small
Model	ViT-B/32
Train compute (MACs)	9.5×10^{16}
Pool size	12.8M
# samples seen	12.8M
Batch size	4096
Training batches	3125
k	2800
Learning rate	5×10^{-4}
AdamW β_1	0.9
AdamW β_2	0.98
AdamW ϵ_{root}	1×10^{-17}
Warmup	500

Our experiments are also run on an incomplete subset of the entire DataComp candidate pool. DataComp did not store the raw image and text files when assembling their dataset; they only stored a list of URL’s to download data from. Due to the nature of the internet, for various reasons, some of these URL’s no longer point to the same data (or no longer point to any data at all). Thus, after ignoring these broken links, our candidate pool is only around 80% of the size of the original DataComp candidate pool when it was collected in 2023. All our results are obtained by running our methods on this subset of the DataComp pool.

Evaluation tasks. In order to ensure that our method is truly improving trained models’ performances on the *entire target distribution* and not overfitting to the target set, for each of the 38 evaluation tasks used by DataComp, we attempted to separately create a disjoint target and validation set (DataComp only creates test sets for each task). Thus, metagradients were computed on the target sets and model performance was evaluated on the validation set, before submitting with the official DataComp script and evaluating on the test sets. This ensures that our method’s generalization ability is being evaluated, and we are not overfitting to our target set.

For various reasons, creating target splits was not possible for all 38 tasks; we summarize our setup in Table 2.

Table 2: All DataComp evaluation tasks. The “Target set” column refers to whether metagradients were taken on the target set corresponding to this dataset.

Dataset	Task	Test size	Train size	Val size	Main metric	Target set
Caltech-101 [FFP04]	Object recognition	6085	2754	306	mean per class	✓
CIFAR-10 [Kri09]	Visual recognition	10000	45000	5000	accuracy	✓
CIFAR-100 [Kri09]	Visual recognition	10000	45000	5000	accuracy	✓
CLEVR Counts [JHV+17; ZPK+19]	Counting	15000	65000	5000	accuracy	✓
CLEVR Distance [JHV+17; ZPK+19]	Distance prediction	15000	65000	5000	accuracy	✓
Country211 [RKH+21; TSF+16]	Geolocation	21100	37980	4220	accuracy	✓
DTD [CMK+14]	Texture classification	1880	3384	376	accuracy	✓
EuroSAT [HBD+19; ZPK+19]	Satellite imagery recognition	5400	19440	2160	accuracy	✓
FGVC Aircraft [MRK+13]	Aircraft recognition	3333	6001	666	mean per class	✓
Food-101 [BGV14]	Food recognition	25250	70750	5000	accuracy	✓
GTSRB [SSS+11]	Traffic sign recognition	12630	35289	3920	accuracy	✓
ImageNet 1k [DDS+09]	Visual recognition	50000	1276167	5000	accuracy	✓
ImageNet Sketch [WGX+19]	Visual recognition	50889	N/A	N/A	accuracy	*
ImageNet V2 [RRS+19]	Visual recognition	10000	N/A	N/A	accuracy	*
ImageNet-A [HZB+19]	Visual recognition	7500	N/A	N/A	accuracy	*
ImageNet-O [HZB+19]	Visual recognition	2000	N/A	N/A	accuracy	*
ImageNet-R [HBM+20]	Visual recognition	30000	N/A	N/A	accuracy	*
KITTI distance [GLU12; ZPK+19]	Distance prediction	711	N/A	N/A	accuracy	†
MNIST [LeC98]	Digit recognition	10000	55000	5000	accuracy	✓
ObjectNet [BMA+19]	Visual recognition	18574	N/A	N/A	accuracy	*
Oxford Flowers-102 [NZ08]	Flower recognition	6149	1836	204	mean per class	✓
Oxford-IIIT Pet [PVZ+12; ZPK+19]	Pet classification	3669	3312	368	mean per class	✓
Pascal VOC 2007 [EVW+10]	Object recognition	14976	14096	1566	accuracy	✓
PatchCamelyon [VLW+18; ZPK+19]	Metastatic tissue cls.	32768	289912	5000	accuracy	✓
Rendered SST2 [ZPK+19]	Sentiment classification	1821	7013	779	accuracy	✓
RESISC45 [CHL17; ZPK+19]	Satellite imagery recognition	6300	22680	2520	accuracy	✓
Stanford Cars [KSD+13]	Vehicle recognition	8041	7329	814	accuracy	✓
STL-10 [CNL11]	Visual recognition	8000	4500	500	accuracy	✓
SUN-397 [XHE+10]	Scene recognition	108753	N/A	N/A	accuracy	‡
SVHN [NWC+11; ZPK+19]	Digit recognition	26032	68257	5000	accuracy	✓
iWildCam [BAC+21; KSM+20]	Animal recognition	42791	147084	5000	macro F1 score	✓
Camelyon17 [BGM+18; KSM+20]	Metastatic tissue cls.	85054	365900	5000	accuracy	✓
FMoW [CFW+18; KSM+20]	Satellite imagery recognition	22108	103261	5000	worst-region acc.	✓
Dollar Street [RDK+22]	Object recognition	3503	13842	1537	worst-income top-5 acc.	✓
GeoDE [RLZ+24]	Object recognition	12438	44488	4943	worst-region acc.	✓
Flickr30k [YLH+14]	Image and text retrieval	31014	N/A	N/A	R@1	§
MSCOCO [LMB+14]	Image and text retrieval	5000	N/A	N/A	R@1	§
WinoGAViL [BBY+22]	Commonsense association	3563	N/A	N/A	Jaccard score	§

*No train or val set exists for this dataset, so we were unable to create disjoint target and val sets.

†We were unable to use this dataset due to technical difficulties.

‡Both the train and val sets were used by DataComp to make their test set, so we were unable to create disjoint target and val sets.

§Retrieval tasks were not used for metagradients.

D Selecting IFT data

In this section, we describe the details of the IFT setting of Xia et al. [XMG+24], as well as the details of our method.

Setting. The setting contains a fixed data pool: instruction fine-tuning data from a data pool consisting of four combined IFT datasets (cf. Table 4 and Xia et al. [XMG+24] for more information). The goal is to select the data that yields the best possible task performance for a LoRA fine-tuning run. We adapt a LoRA to a Gemma-2B model (the pretraining-only Gemma-2B model) using the LoRA configuration from Xia et al. [XMG+24].

Data splits. See Table 3 for a description of the available data for each task, along with the task setup details. Xia et al. [XMG+24] constructed these extra samples by drawing from the ICL samples given in the tasks originally. Note that we drop TydiQA from the original work of Xia et al. [XMG+24] as there are not enough samples to select with (there is only one from each category, for a total of 7).

Method. We execute Algorithm 1 with k as 150 steps from the end of training and the Bernoulli parameter p controlling the step size as 0.2. At each step, we choose a “minibatch” with a size equal to half the target set and a quarter of the target set for BBH and MMLU, respectively (that is, we only select to optimize performance on a fraction of the target set at a time). We model select over iterates and hyperparameters by (a) choosing the top three steps in terms of validation loss for each run (b) selecting the best one in terms of full train set accuracy (including the part that we trained on). We perform this procedure—akin to Pareto optimization [JS08]—because the validation set is so small (as the overall set of samples is very small) that it is difficult to select models without overfitting otherwise.

We compare with two baselines: training on the full dataset (i.e., training on the entirety of all the data for a single epoch), and LESS (we use the data selected according to “LESS-T” [XMG+24], following the recommendation of 4 epochs).

For model training, we train with ADAM ($\beta_1 = 0.95, \beta_2 = 0.975$, decoupled weight decay as 10^{-5}) and a one-cycle linear schedule starting at 10^{-6} of the maximum learning rate, reaching the peak over 25% of training, then ending at 0.1 of the maximum learning rate. We insert a positive $\varepsilon_{\text{root}}$ into the inverse square root term in the ADAM update to prevent metagradient (and to a lesser extent update) blowup (see Eq. 12). The model training is the same across selected data, except that we use $\varepsilon_{\text{root}} = 10^{-7}$ for MGD-selected data and $\varepsilon_{\text{root}} = 10^{-9}$ for the other runs (we select the optimal parameter for each class of method). We additionally hyperparameter select for the best learning rate across each baseline by minimizing validation set loss; LESS performs best with a smaller learning rate (0.00024 for BBH and 0.00012 for MMLU) than training on the full dataset or with MGD (0.0006 for both). We normalize the loss of each training sample by taking the mean across predicted tokens during training, and do not divide by the batch size (important for scaling the $\varepsilon_{\text{root}}$ term, but otherwise ADAM is invariant to the scale).

Selecting smooth model training for MGD. For MGD runs, we jointly select learning rate and $\varepsilon_{\text{root}}$ using the smoothness metric of Section 3. We find that the choice of $\varepsilon_{\text{root}}$ term is important (just as the choice of ε is important in standard ADAM training); choosing a much larger term results in non-smooth training. We also find that metagradints are sensitive to learning rate schedule; choosing a much larger or smaller maximum learning rate results in non-smooth training.

Table 3: Overview of datasets used in IFT dataset selection (from Xia et al. [XMG+24]).

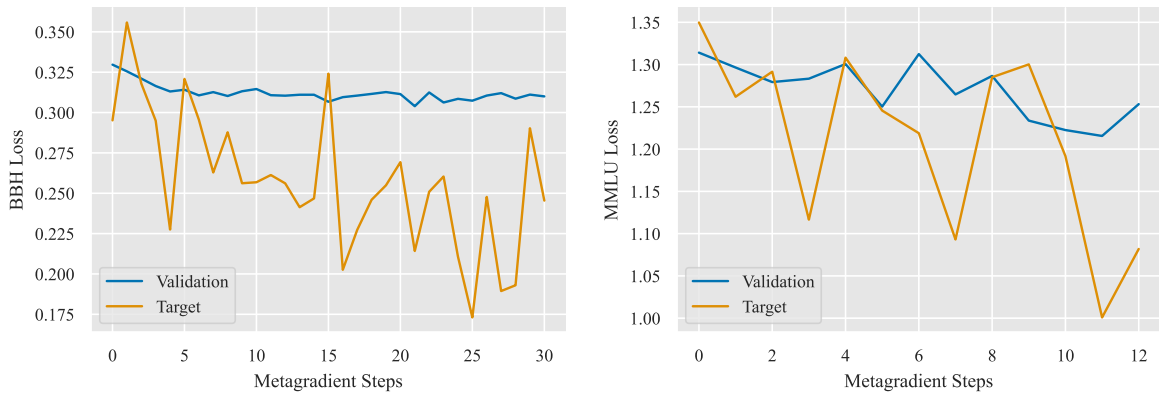
Dataset	# Shot	# Tasks	n_{target}	n_{val}	n_{test}	Answer Type	Type of Task
MMLU	5	57	57	228	18,721	Letter options	Knowledge/Recall
BBH	3	23	23	46	920	COT and answer	Reasoning

Table 4: Details of IFT training datasets.

Dataset	# Instance	Sourced from	Prompt Len.	Completion Len.
FLAN V2	100,000	NLP datasets and human-written instructions	355.7	31.2
CoT	100,000	NLP datasets and human-written CoTs	266	53.2
Dolly	15,011	Human-written from scratch	118.1	91.3
Open Assistant 1	55,668	Human-written from scratch	34.8	212.5

IFT results

Figure 13: MGD dataset selection improves the validation loss over metagradient steps, demonstrating our method’s efficacy. However, the gap between loss on samples MGD directly optimizes on and the validation samples widens over the number of iterates, and there is overfitting depending on the number of steps taken.



E Accuracy-degrading data poisoning

E.1 Background on Gradient Cancellation attack

We briefly review the Gradient Cancellation attack [LKY23] used as a baseline in our experiments. We refer the reader to the original paper for details. Here we highlight the key ideas.

At a high level: Gradient Cancellation (GC) explicitly aims at making a specific malicious parameter configuration reachable through retraining on the poisoned dataset. The attack operates in two phases:

1. **Parameter Generation:** The attacker generates a target malicious model parameter independently, often using a direct parameter corruption method like Gradient-based Parameter Corruption (GradPC) [LKY23]. The end result of this phase is a target model parameter θ_p that achieves low accuracy on the test set, but is close to the original parameter θ_0 derived from training on the clean dataset.
2. **Poison Data Crafting:** In the second phase, GC finds values of the poison data that induce a near-zero gradient at the target parameter θ_p . This is achieved by solving a gradient cancellation optimization problem: specifically, GC minimizes the total gradient of the loss function (with respect to the model parameters) evaluated over the combined (clean and poisoned) dataset, aiming to ensure that the gradient at the malicious parameter θ_p approaches zero.

E.2 Metasmooth hyperparameters

Table 5: Hyperparameters used in the ResNet-9 [Jor24] CIFAR-10 poisoning experiments. The augmentations used are normalization, random horizontal flip, and random translate (2 pixels)

Hyperparameter	Value
Learning rate	0.5
β_1	0.85
Weight decay	10^{-5}
Exclude BatchNorm	True
Optimizer	SGD
Batch size	250
Epochs	18
Starting learning rate fraction	0.5
Relative min. learning rate	10000
Scheduler max. iterations	50000
Nesterov momentum	True
BatchNorm ϵ	10^{-5}
BatchNorm momentum	0.5
Final bias	True
Width multiplier	2.0
Final scale	0.125
Initial scale	2.0
Batchnorm location	Before activation
Activation function	GELU
Pooling type	Average
Test-time augmentation	True

F LR optimization

Table 6: The grid search was run over all 528 combinations of the hyperparameter values below.

Parameter	Values
Peak learning rate	[7.0, 7.5, 8.0, 8.5, 9.0, 9.5, 10.0, 10.5, 11.0, 11.5, 12.0]
Initial LR multiplier	[0.05, 0.15, 0.25, 0.35, 0.45, 0.55]
Final LR multiplier	[0.05, 0.15, 0.25, 0.35, 0.45, 0.55]
LR peak time	[0.25, 0.5, 0.75]

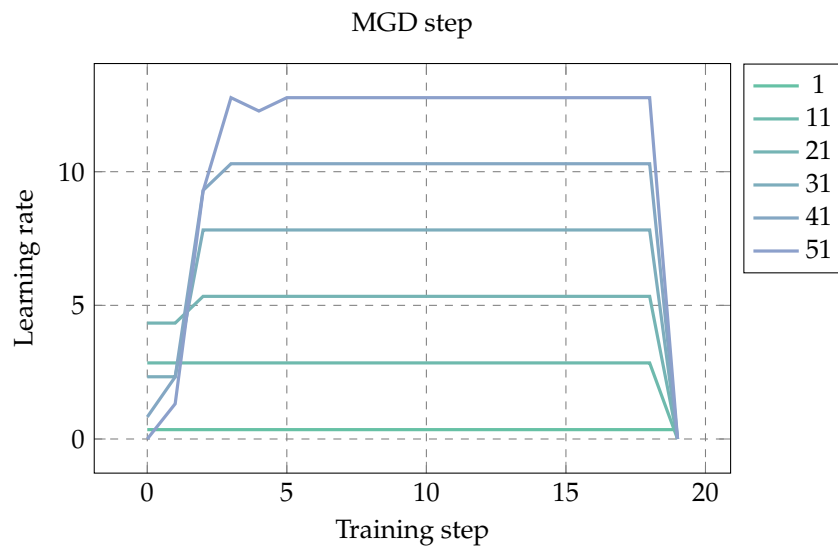


Figure 14: Graphs of our learned LR schedules.